Measurements of coronal fields met by CME-driven shocks and determination of 3D CME kinematic

A. Bemporad

INAF-Turin Astrophysical Observatory, Italy

INAF – Italian National Astrophysics Institute

OATo – Turin Astro-physical Observatory

Outline

• FIRST PART: pre- and post-shock coronal field measurements with WL and UV observations

• SECOND PART: determination of 3D information on CMEs from polarization-ratio technique

• THIRD PART: other diagnostic capabilities for study of solar eruptions

FIRST PART:

pre- and post-shock coronal field measurements with WL and UV observations

Recent coronal field measurements from space

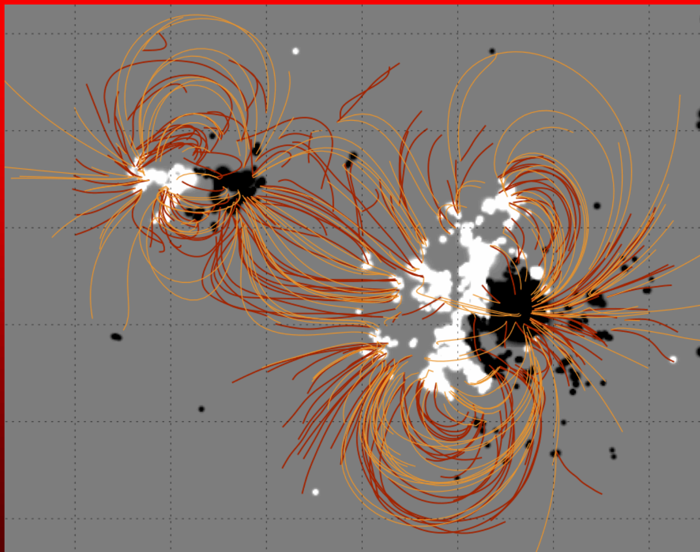

Comparison between unipolar potential field extrapolations (orange) and 3D reconstructed loops (red) → significant differencess in loop inclination and connectivities

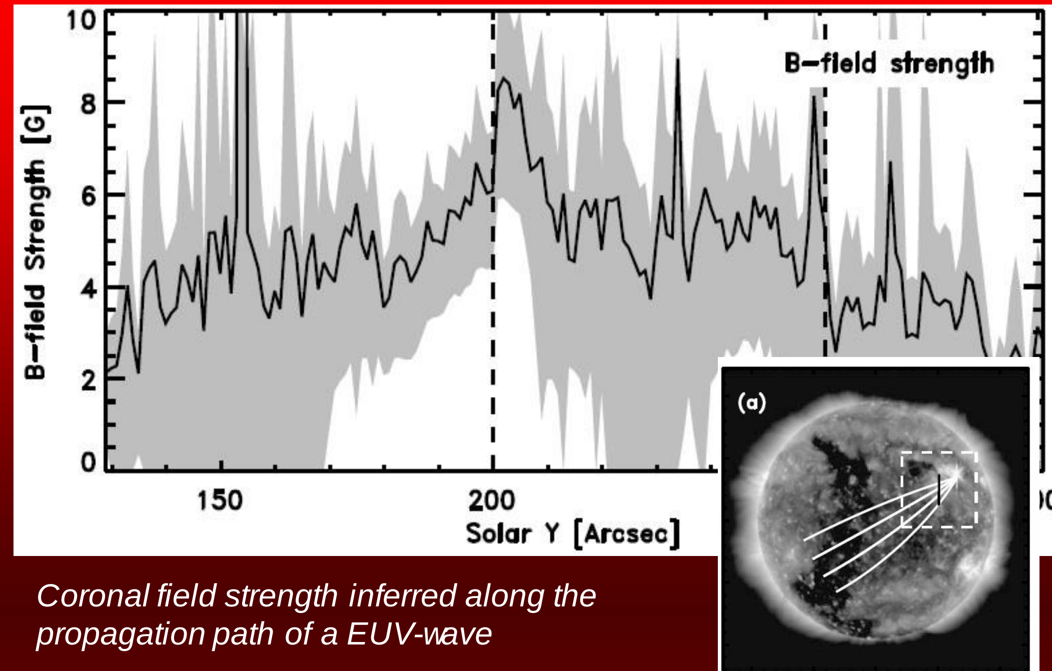

Coronal field strength inferred along the propagation path of a EUV-wave

- **Field extrapolations bounded to 3D stereoscopic reconstructions**: forward fitting of 3D loops with multipolar photospheric dipole-fields → disagreement due to non-potentiality and currents, but also to inadequacy of photospheric magnetograms.

(De Rosa et al. 2009; Aschwanden et al. 2012; Chifu et al. 2015)

- **Field strength from propagation of EUV-waves**: by assuming that EUV-wave speed = fast magnetosonic speed and measuring the coronal density and temperature from EUV images/spectra (AIA + EIS data) → need a comparison with extrapolated field to infer height estimates

(Long et al. 2011; West et al. 2011)

Recent coronal field measurements from ground

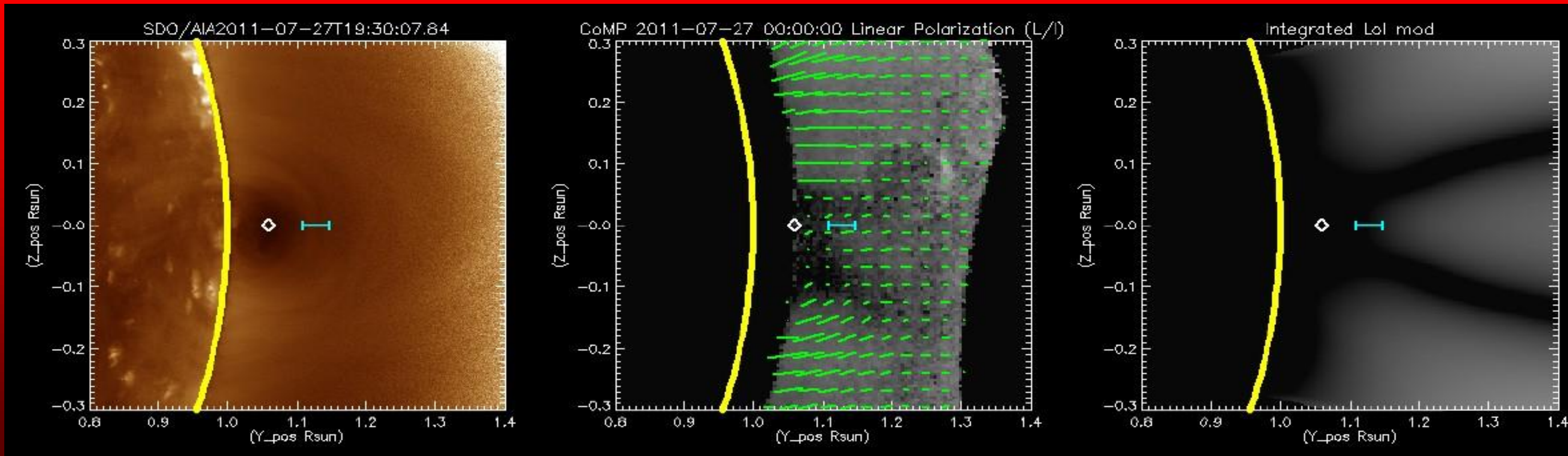

Example (courtesy of S. Gibson) of a coronal cavity observed by SDO/AIA 171 (left), and the characteristic "V-shaped" Van Vleck signatures in the distribution of the FeXIII 1074nm linear polarization strength as observed (middle) and simulated (right)

Different instruments (e.g.: CoMP, CoMP-S, CorMag) are now providing unique information on coronal fields via:

- **Zeeman effect** on VIS/IR spectral lines (e.g. FeXIII 1074nm) → spectro-polarimetry provides: a) measurements of circular polarization (Stokes V/I) → **B line of sight strength**; b) measurements of linear polarization (Stokes L/I) becoming 0 at Van Vleck angle (~54° between the radial and local field orientation) → **B orientation on the plane of the sky**;
- **Hanle effect** (saturated $A_{ij} < v_B$) on VIS spectral lines (e.g. FeXIV 530nm), spectro-polarimetry provides measurements of linear polarization → **B orientation on the plane of the sky.**

Issues related with LOS integration will be solved via tomographic-inversion once daily obs. will be available (ATSA, COSMO, ASPIICS), assuming stationarity of coronal structures.

Coronal field measurements with Shocks

A new technique to **measure coronal fields crossed by CMEs** proposed by Gopalswamy & Yashiro (2011) by applying the Furris & Russell's (1994) relation between the **standoff distance** ΔR of an interplanetary shock and the radius of curvature R_c of the driver:

$$M_{\Delta R}^2 = \frac{\Delta R / R_C(\gamma+1)+1.6}{\Delta R / R_C(\gamma+1)-0.8(\gamma-1)}$$

(Kim et al. 2012)

$\Delta R = R_{shock} - R_{fluxrope}$, M = shock Mach number, γ adiab. index.
Technique: measure R_{shock} *and* $R_{fluxrope}$ from WL images → estimate of $M = v_{in}/v_A = (v_{shock} - v_{solarwind})/v_A$ → measure v_{shock} and assume $v_{solarwind}$ → estimate of $v_A = B/(\mu\rho)^{0.5}$ → measure ρ (from pB images or type-II radio burst) → **estimate of *B***.

→ applied to shocks observed in WL coronagraphic images (Kim et al. 2012), **EUV disk imagers** (Gopalswamy et al. 2012) and **WL Heliospheric imagers** (Poomvises et al. 2012).

Limits: field can be measured only at the nose where quasi-parallel shock can be assumed

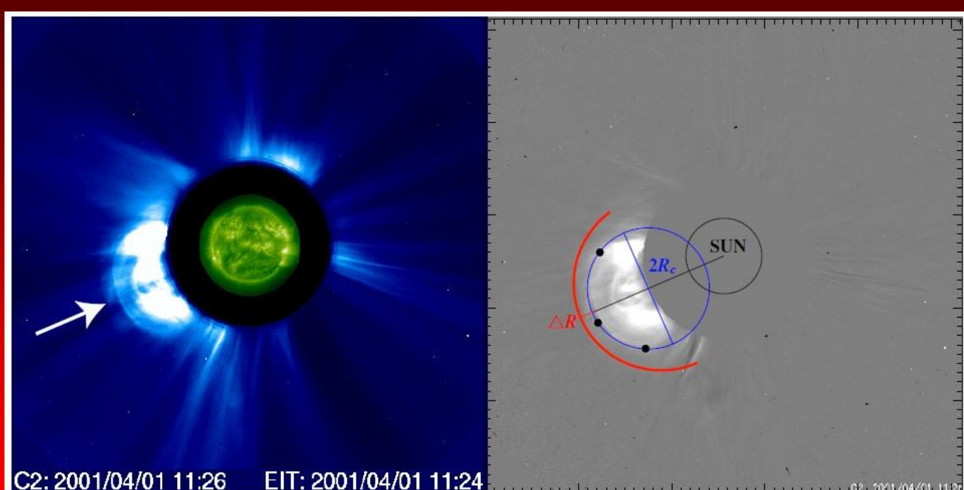

(Kim et al. 2012)

Alternatively coronal field can be measured directly from the **density compression ratio *X*** at the shock front:

$$M_{\rho}^2 = \frac{2X+\gamma+1}{\gamma+1-X(\gamma-1)}$$

Results: B and v_A measured in a wide range, B consistent with previous measurements.

Problem: shock **compression ratios X from WL likely underestimated** by a factor of ~ 2 because of LOS assumptions.

Results from combined WL and UV data

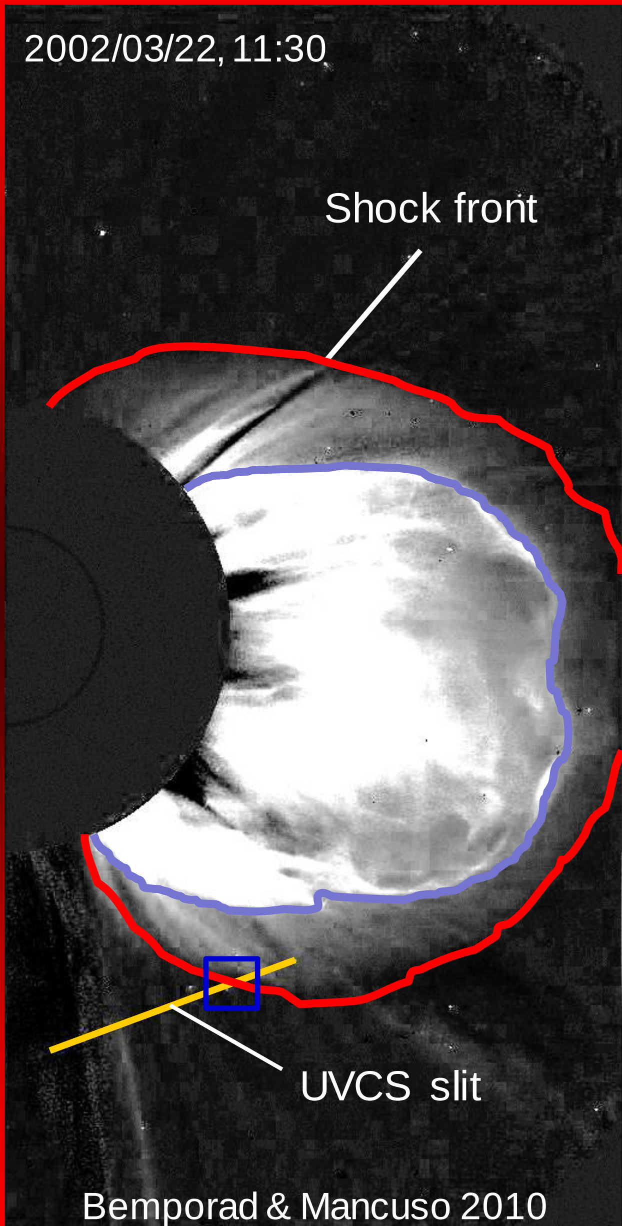

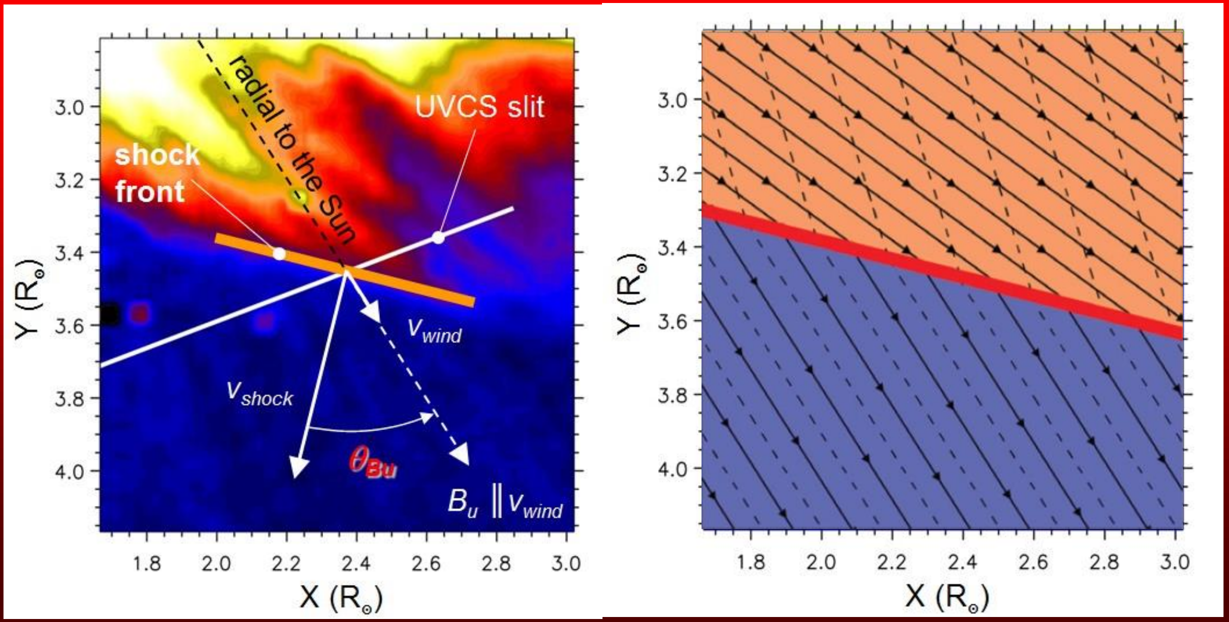

Bemporad & Mancuso (2010)

MHD Rankine-Hugoniot eq. can be rewritten so that:

$$\begin{bmatrix} T_u, n_u, v_u, \\ \vartheta_{Bu}, \vartheta_{vu}, r \end{bmatrix} \rightarrow \text{Rankine-Hugoniot eq.} \rightarrow \begin{bmatrix} B_u, T_d, B_d, \\ v_d, \vartheta_{Bd}, \vartheta_{vd} \end{bmatrix}$$

Detection of shock in UV and WL → MHD-Rankine Hugoniot eq. for oblique shock → X (~2), heating factor (~8), ***B* strength up- & down-stream** (0.019G to 0.037 G), **magnetic and velocity fields rotation** across the shock (~23° and 15°).

Results from combined WL and UV data

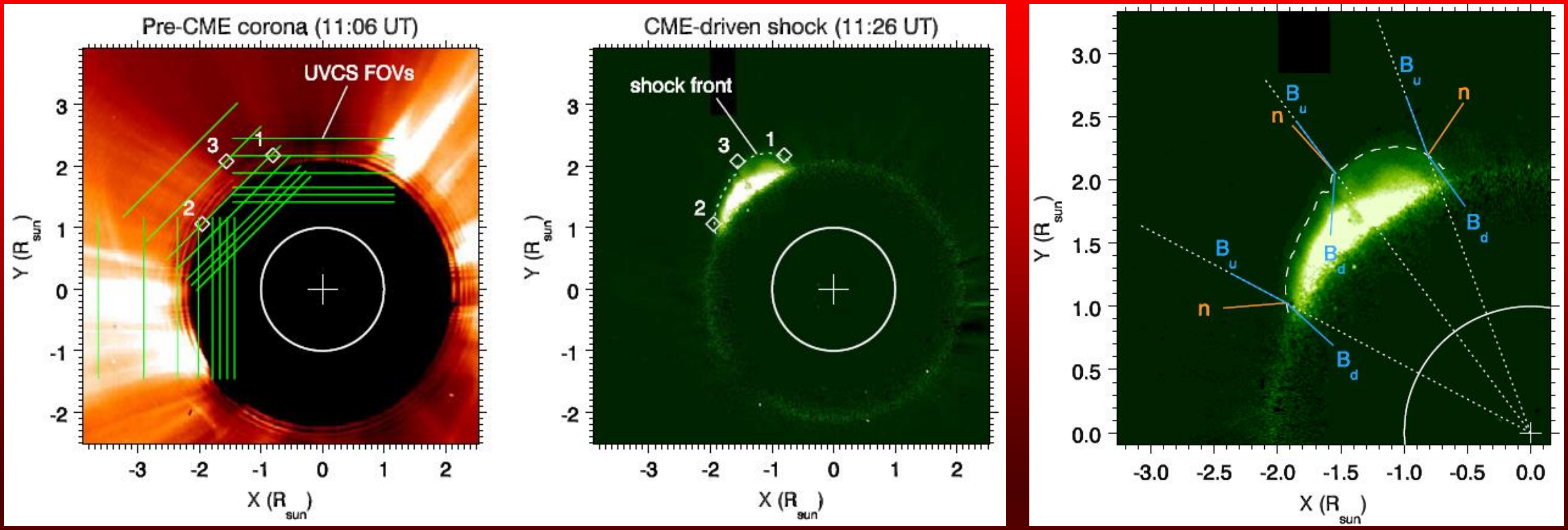

Bemporad, Susino & Lapenta 2014

Unique information on shocked plasma derived from analysis of **both UV and WL data**:

• LASCO + UVCS pre-CME data → **upstream parameters** (T, n, v_{out}), but the magnetic field.
• upstream parameters + shock **compression ratio X** from WL → **R-H equations for oblique shock** → **downstream parameters** including **full B vector** on the plane of the sky.
• **Shock transit** → **compression** (factor ~ 1.7–2.7), **heating** (factor ~ 1.5 – 3.0 at the flanks, ~ 8 – 12 at the nose), ***B* compression** (factor ~ 1.2 – 1.9) & **deflection** (~ 14° – 22° at the flanks, > 40° at the nose). **Heating derived with RH-Eq. more likely represents proton heating**, while temperature increases by adiabatic compression (factor ~2 at the nose, ~1.2–1.5 at the flanks) likely more representative of electron heating → **shock transit → T_e – T_p decoupling**.

Test of results with MHD simulations

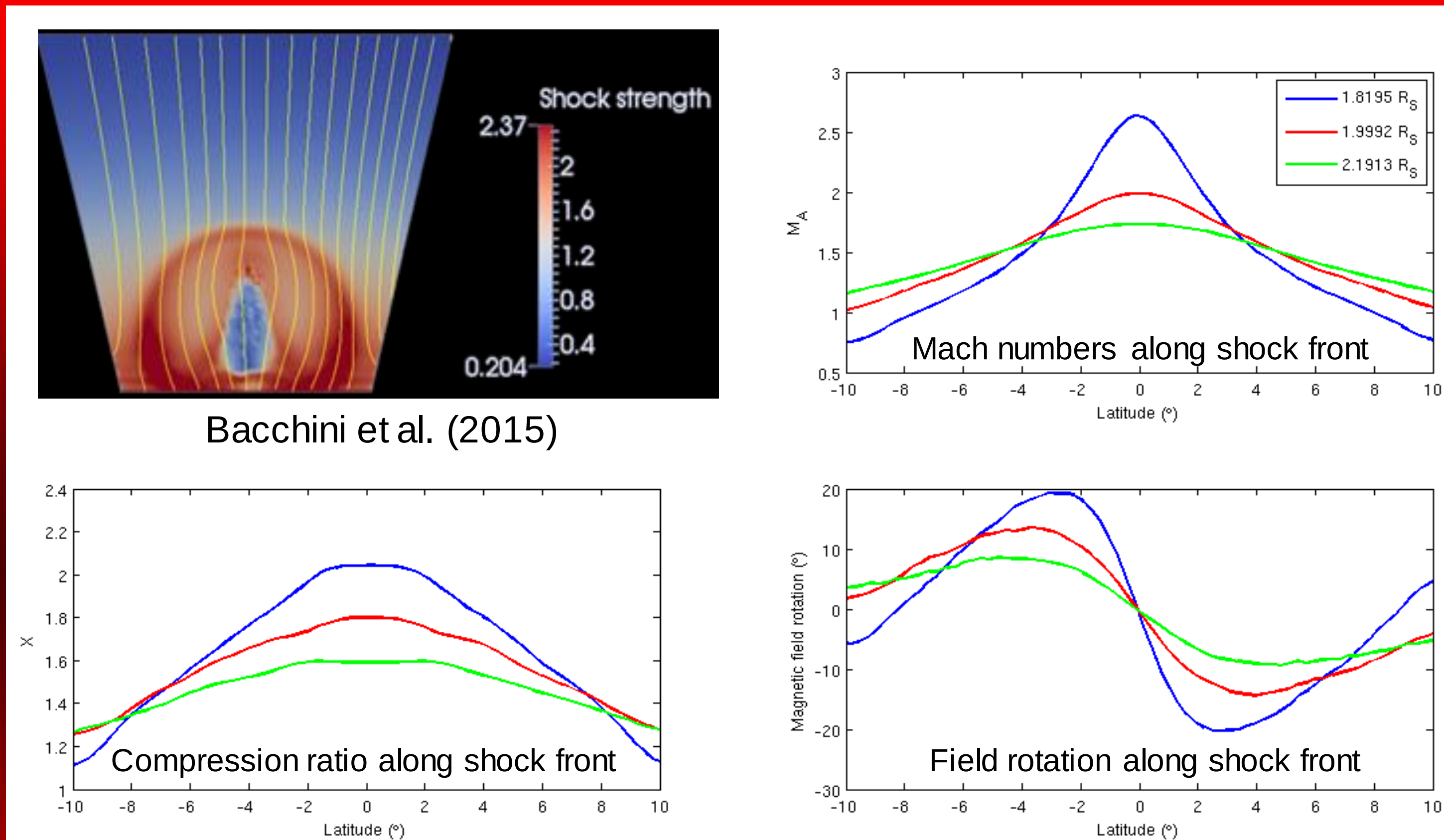

2D single-fluid MHD simulations of a coronal shock were performed (by the Group at CPA–KU Leuven) with FLIPMHD3D (based on Brackbill, 1990).

Results: very **good agreement** between **observations and numerical simulations** for the spatial distribution and time evolution of 1) compression ratios X, 2) Mach numbers M_A, and 3) magnetic field deflections across the shock surface.

The June 7th 2011 eruption

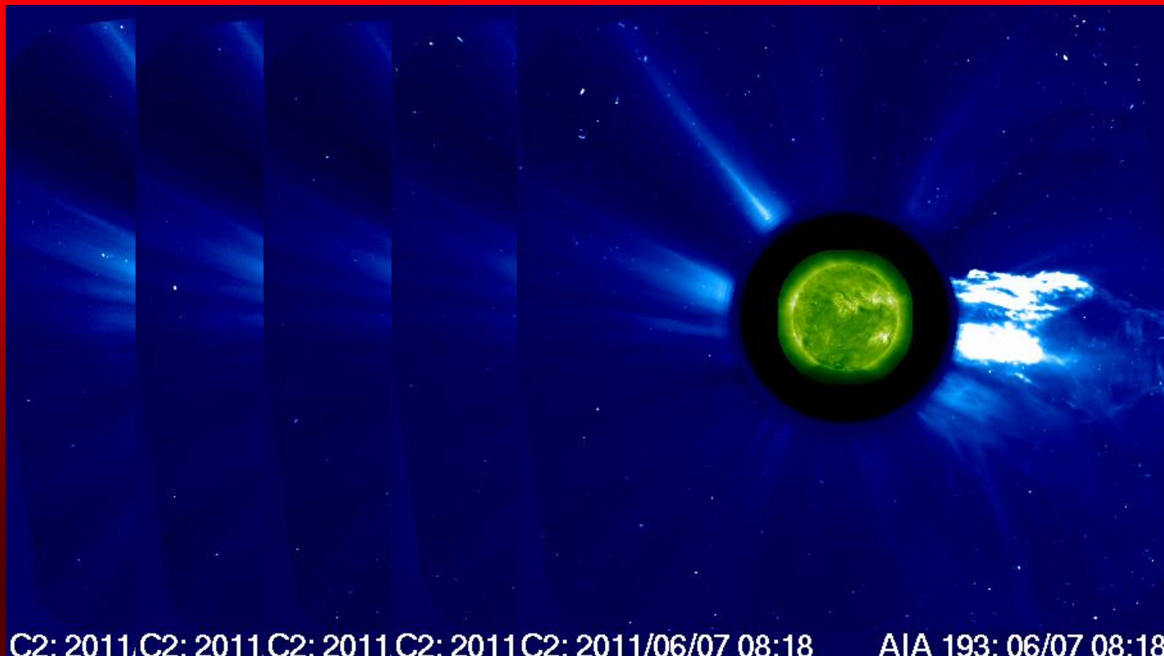

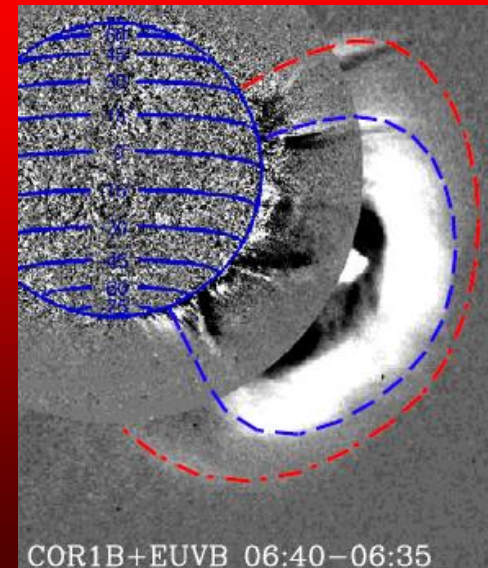

CME bubble and compression front (Cheng et al. 2012).

Spectacular eruption (associated with M2.5 flare, type-II and –III radio bursts, γ-ray emission, Ackermann et al. 2014). Many different works published relative to this eruption focusing on:

- dynamics and plasma properties of **returning plasma blobs** (Carlyle et al. 2014; Dolei, Bemporad & Spadaro 2014; Innes et al. 2012; Williams et al. 2013)
- associated **EUV waves** (Cheng et al. 2012) and **type-II burst** (Dorovskyy et al. 2015)
- energy release from **falling material impact** on the sun (Gilbert et al. 2013; Reale et al. 2013)
- **reconnection driven** by the CME (van Driel-Gesztelyi et al. 2014)

Our analysis focused on the WL data relative to the associated shock wave.

2D maps of coronal fields from WL observation of CME-driven shocks

- Analysis of WL (*pB*) coronal pre-CME image → 2D map of ambient pre-CME coronal densities $\mathbf{n_e}$.
- Identification of shock surface location (pixel by pixel) in WL images →
  - a) shock kinematic → 2D map (altitude vs. latitude) of shock velocity $\mathbf{v_{shock}}$;
  - b) orientation of shock surface with respect to the radial direction → shock inclination angle $\boldsymbol{\vartheta_{shock}}$ at different latitudes.
- Hypothesis on the pre-shock coronal outflow speed v_{wind} → 2D map of shock upstream velocity $\mathbf{v_{up}}$.
- Analysis of WL (*tB*) intensity variation across the shock surface → shock compression ratios $\mathbf{X_{shock}}$ at different altitudes and latitudes
- Hypothesis on the expression of Mach number for the general case of oblique shock (next slide) → 2D map of shock Mach number $\mathbf{M_A}$.
- Combination of M_A and v_{up} 2D maps → 2D map of the upstream Alfvén velocity $\mathbf{v_A}$
- Combination of v_A and n_e maps → **2D map of pre-shock coronal field strength *B* (without application of MHD-RH equations)**

Compression ratios and Mach numbers from WL

- **Pre-shock densities** derived with latest pre-CME LASCO pB image.

- **Compression ratios *X*** derived all along the shock front by:

1. measuring the WL intensity ratio between the front and the corona,
2. taking into account LOS integration effects (shock depth L along the LOS from its projected thickness: L=0.9 $R_\odot$ for C2, 1.1 < L < 1.3 $R_\odot$ for C3),
3. deriving the density in the shocked region reproducing the WL increase.

Results: X maximizes at shock nose, X decreasing with shock altitude.

- **Mach numbers M_A** derived all along the shock front by:

1. measuring from WL images the inclination θ of shock surface with respect to the radial,
2. applying the empirical formula (tested in Bemporad et al. 2014 and Bacchini et al. 2015) for M_A in the case of oblique shock (β << 1, γ = 5/3)

$$M_{A\perp} = \sqrt{\frac{X(X+5)}{2(4-X)}}$$

(Bemporad & Mancuso 2012)

$$M_{A\parallel} = \sqrt{X}$$

$$M_{A\angle} = \sqrt{(M_{A\perp}\sin\theta)^2 + (M_{A\parallel}\cos\theta)^2}$$

Results: M_A maximizes at shock nose, decreasing with shock altitude.

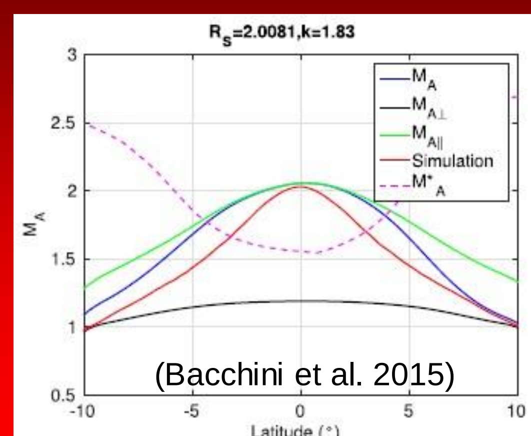

(Bacchini et al. 2015)

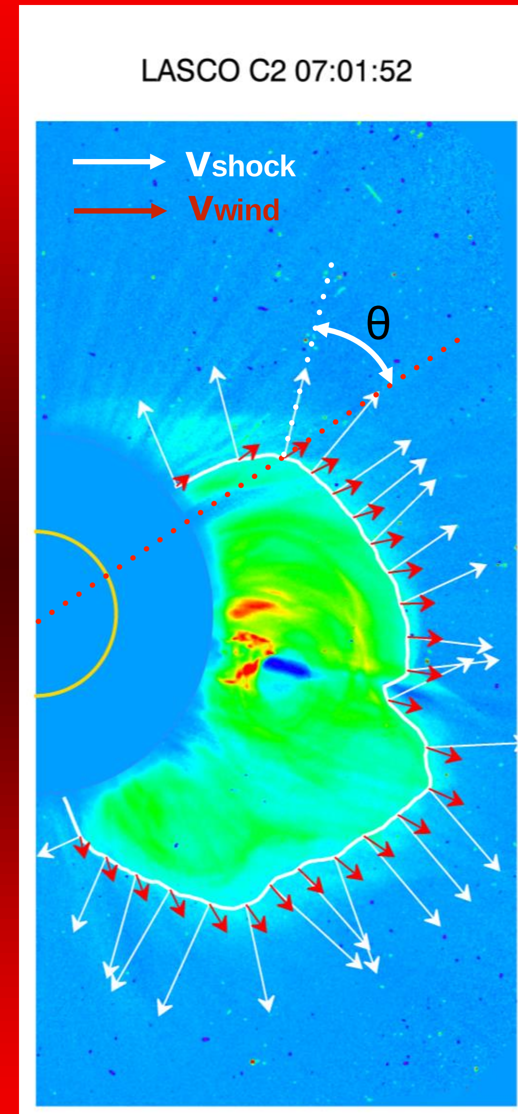

Results: 2D maps of v_{shock}, M_A, v_A, n_e

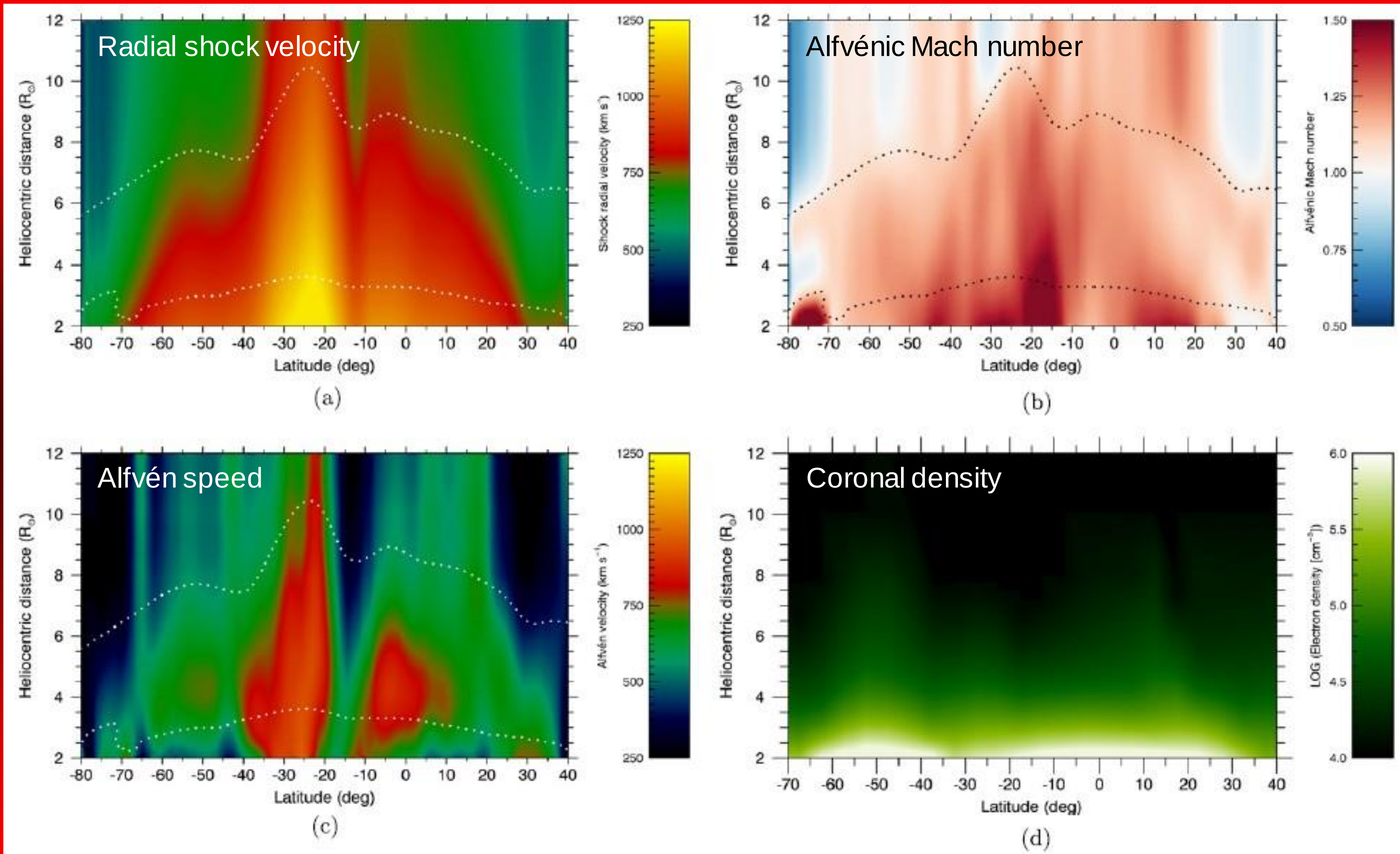

Susino, Bemporad & Mancuso (2015)

Results: 2D map of coronal Magnetic Fields

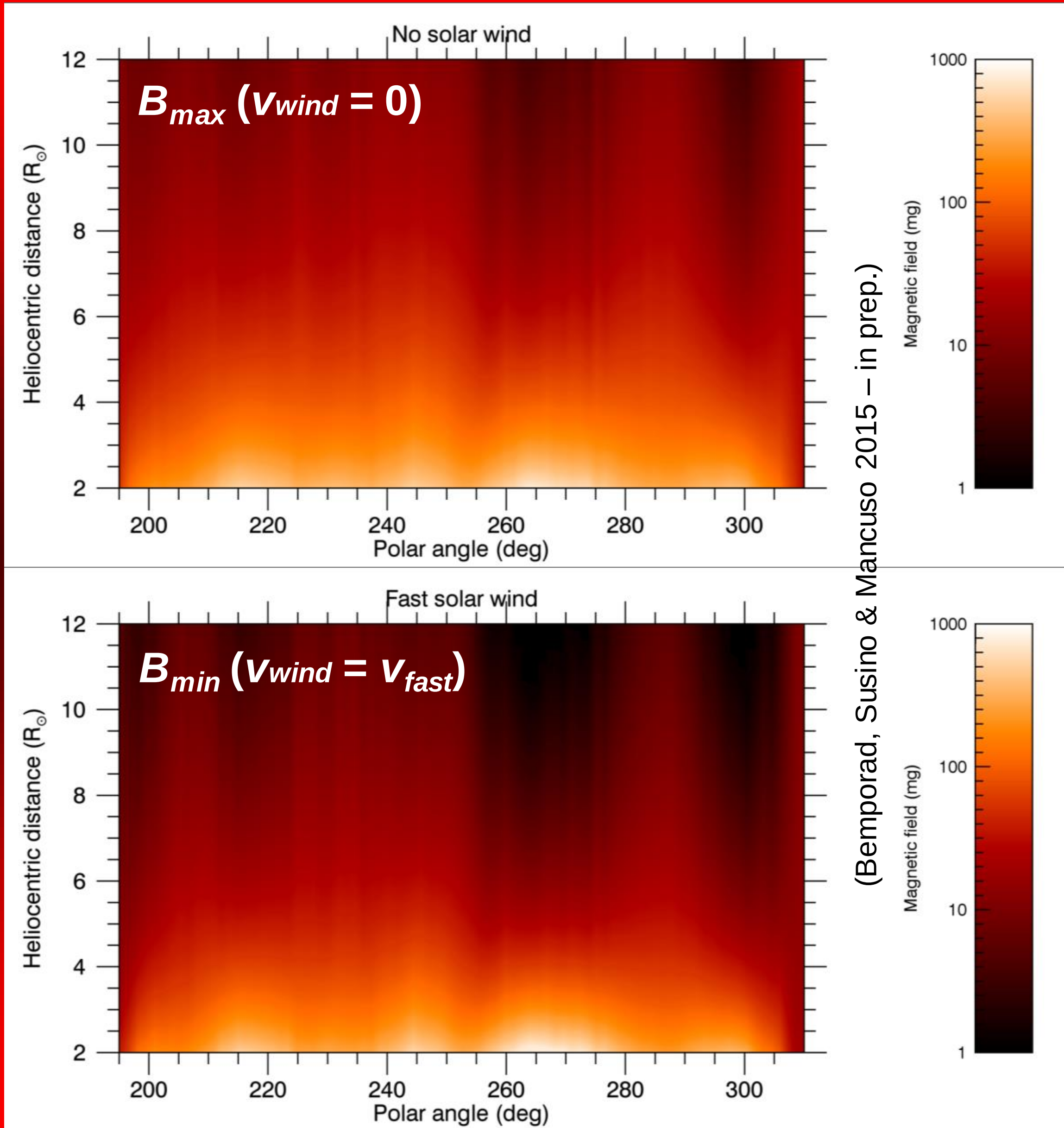

Upstream coronal magnetic field: derived from the Alfvén speed, assuming either **no solar wind** (*B* upper limit) or **fast solar wind** (*B* lower limit) using the model of Hu, Esser & Habbal (1997).

$$B_u = v_A \sqrt{\mu_0 m_p n_e}$$

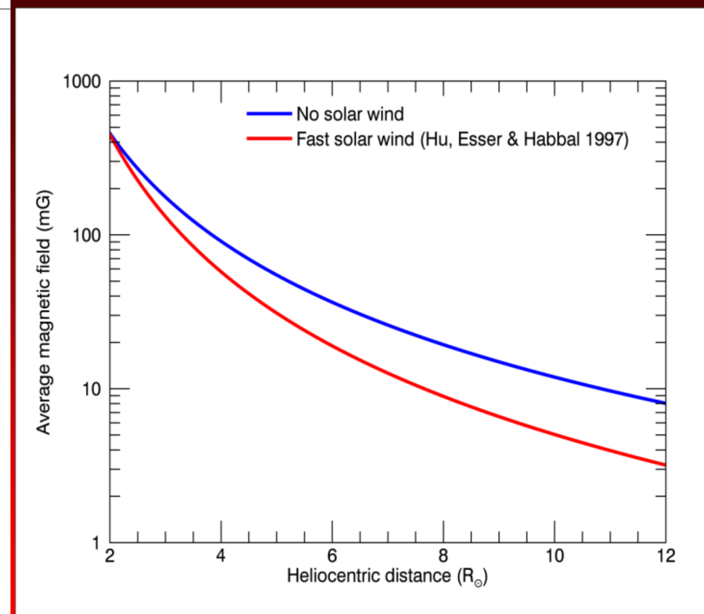

Coronal Magnetic Fields

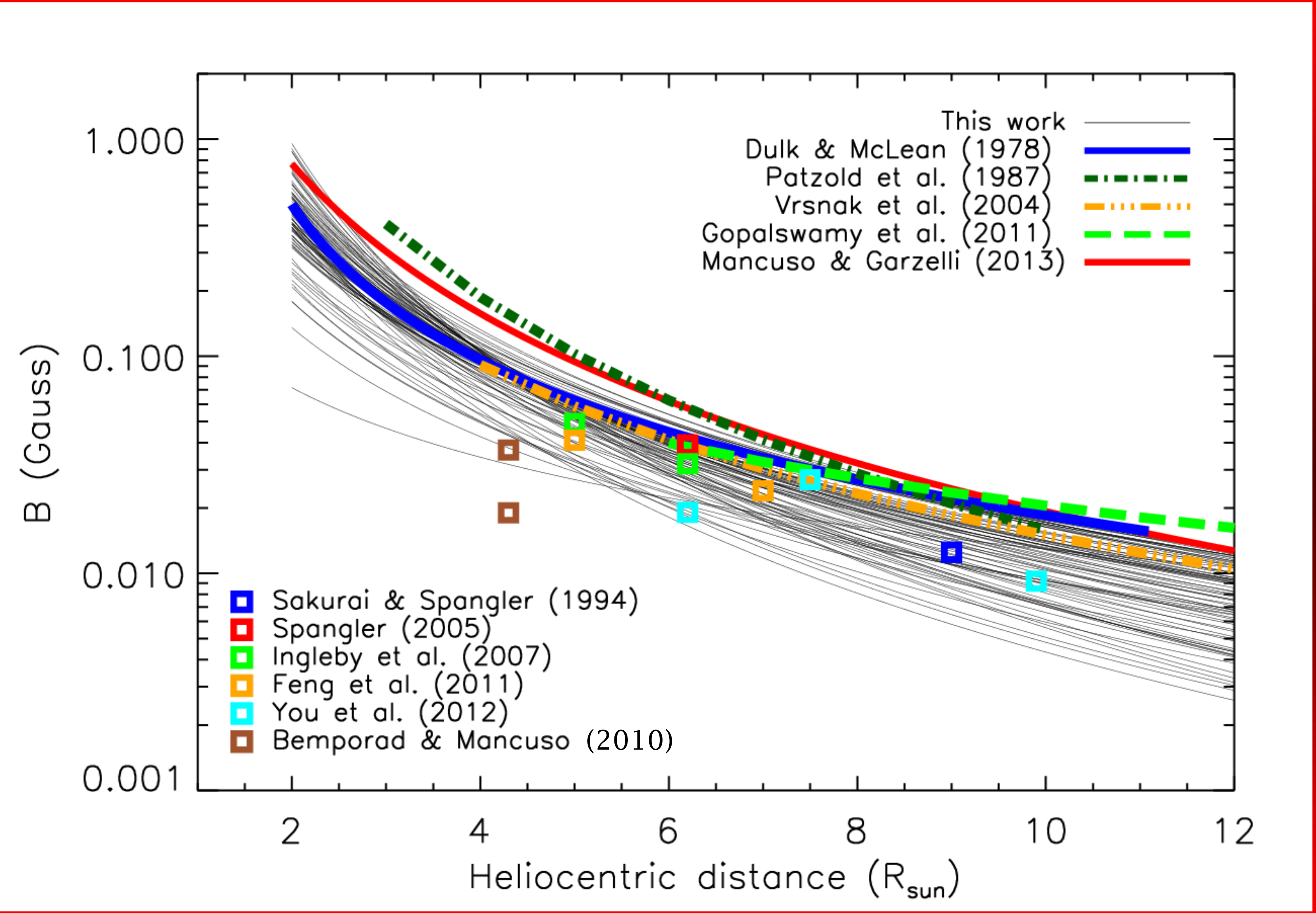

Susino, Bemporad & Mancuso (2015)

Coronal Magnetic Fields

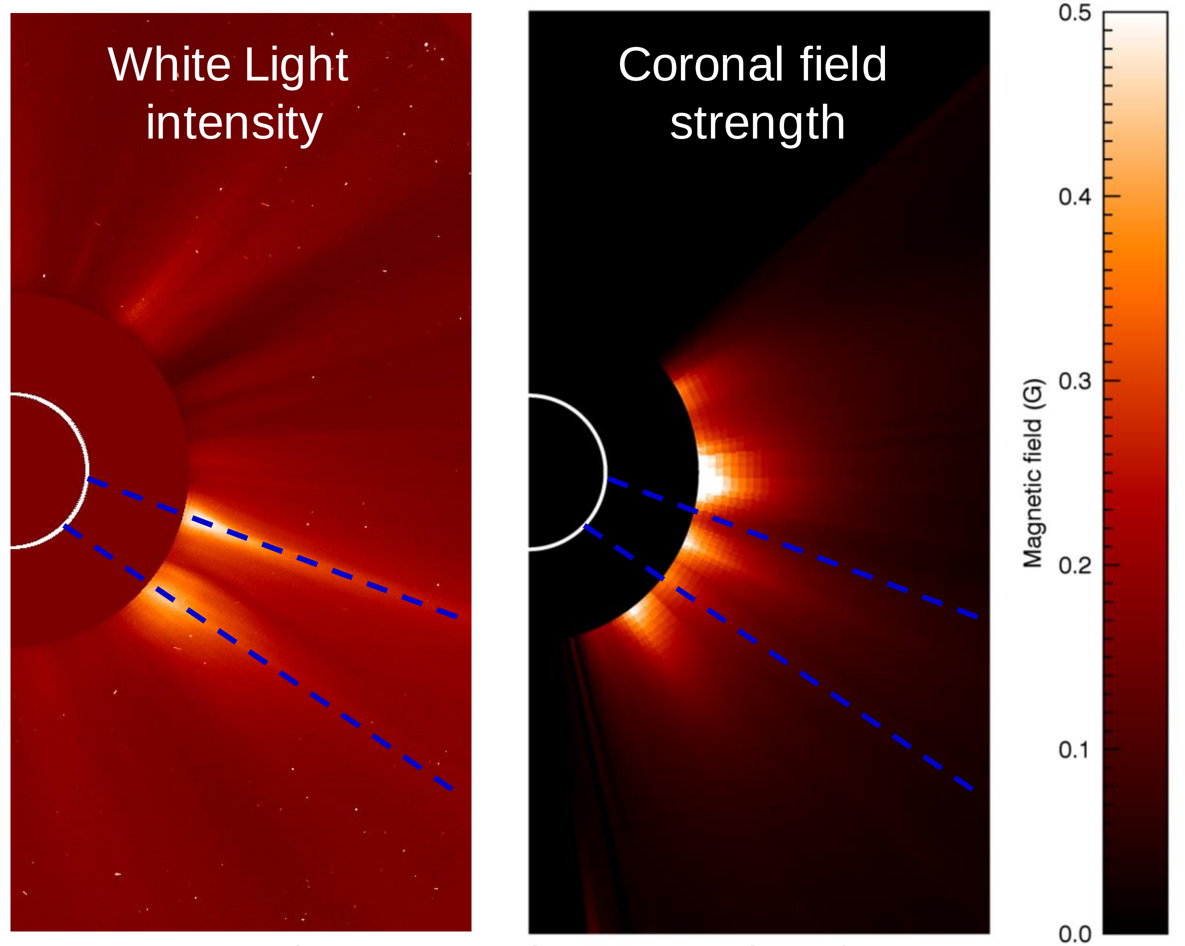

Susino, Bemporad & Mancuso (2015)

<u>Results:</u> brighter features in WL (streamers) associated with lower magnetic field strength and vice-versa → in agreement with the location of neutral CSs.

This is the **first ever 2D coronal magnetic field map derived with such large altitude and latitude coverage**.(~110° in latitude, 12 R_{sun} in altitude)

Future developments (1/2)

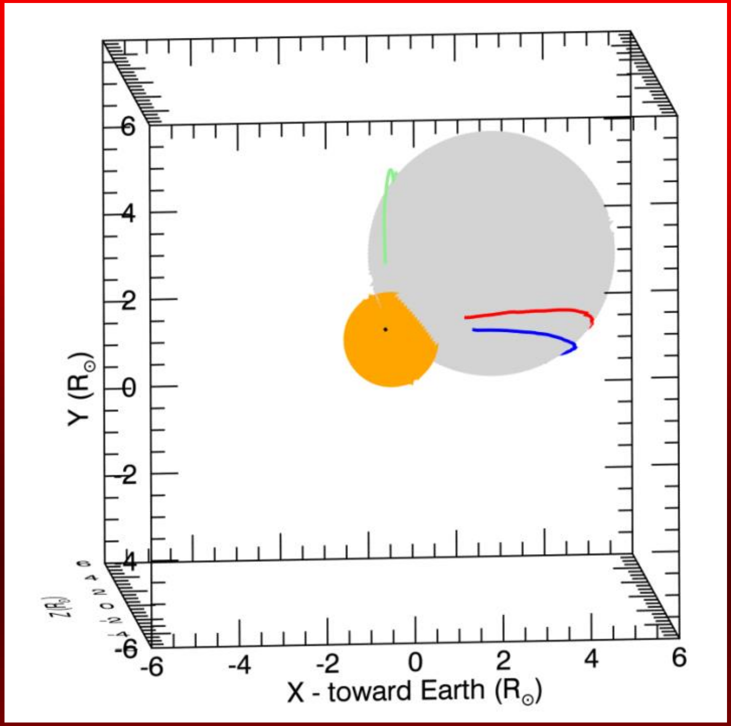

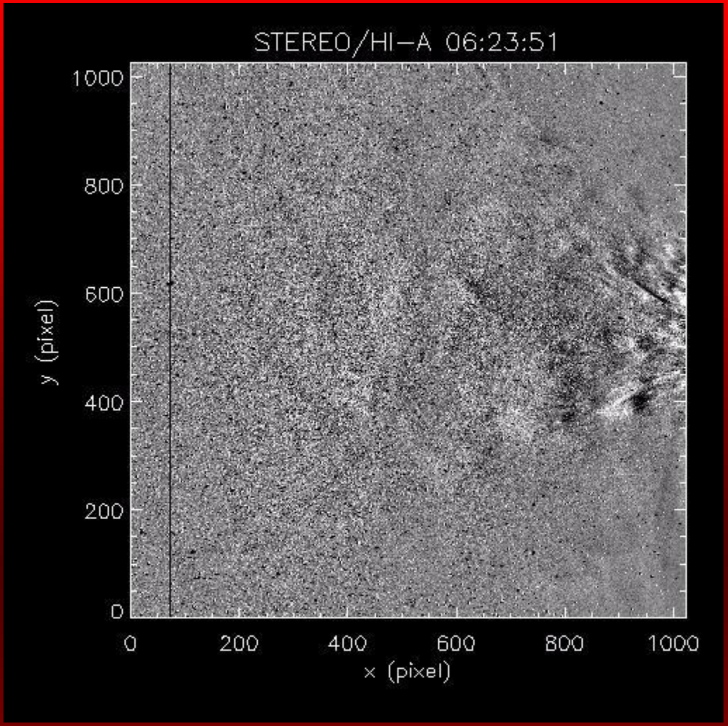

- Identification of **shock front** in COR-A and –B data → **2D maps of mag. fields** in the intermediate corona (~ 2-10 R_{sun}) at **different longitudes** → comparison with field extrap. and 3D MHD models;
- identification of possible **SEP sources** in the corona → **3D reconstruction** of the **shock surface** with LASCO, COR1-A and COR1-B **+** comparison with SEP fluxes measured by SOHO and STEREO + SEP propagation model;
- identification of **interplanetary shock** in HI data → determination of 2D maps of magnetic fields in the outer corona.

Future developments (2/2)

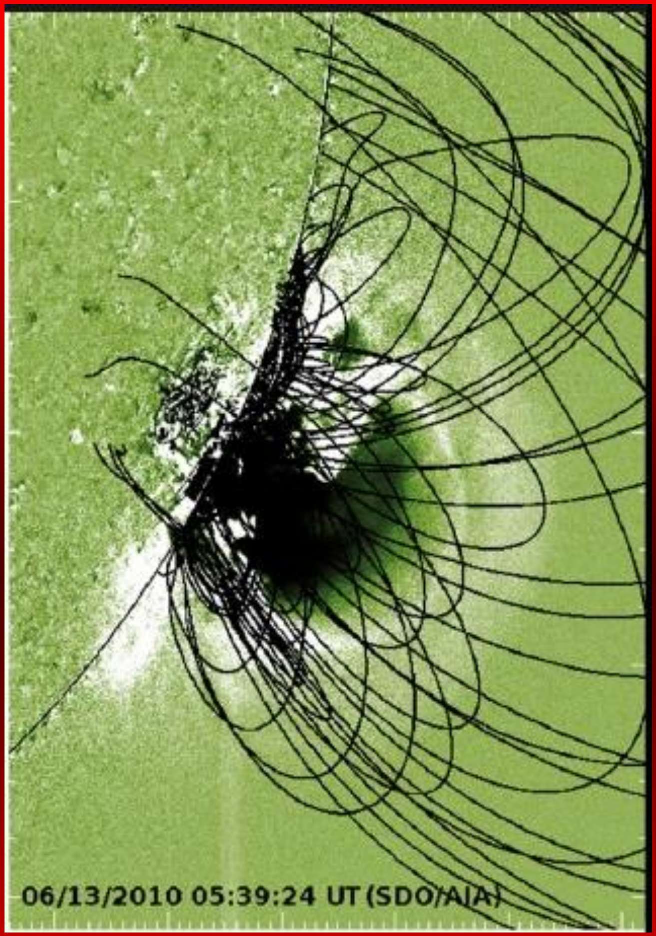

Kozaref et al. (2011)

QUESTION 1: can we use these techniques for space weather predictions?

Select good candidate events for the determination of **lower coronal field strenght, compression & deflection** (**WG5 – Bs challenge**) across the shock from the early evolution in EUV images; this will need:

- inclusion of a coronal field extrapolation/model for the pre-shock field orientation,
- inclusion of pre-shock coronal field orientation as observed with spectro-polarimetry (CoMP data),
- comparison between magnetic field strengths measured with shock and spectropolarimetry and extrapolated field,
- discuss how results are related on the assumed pre-shock field inclination.

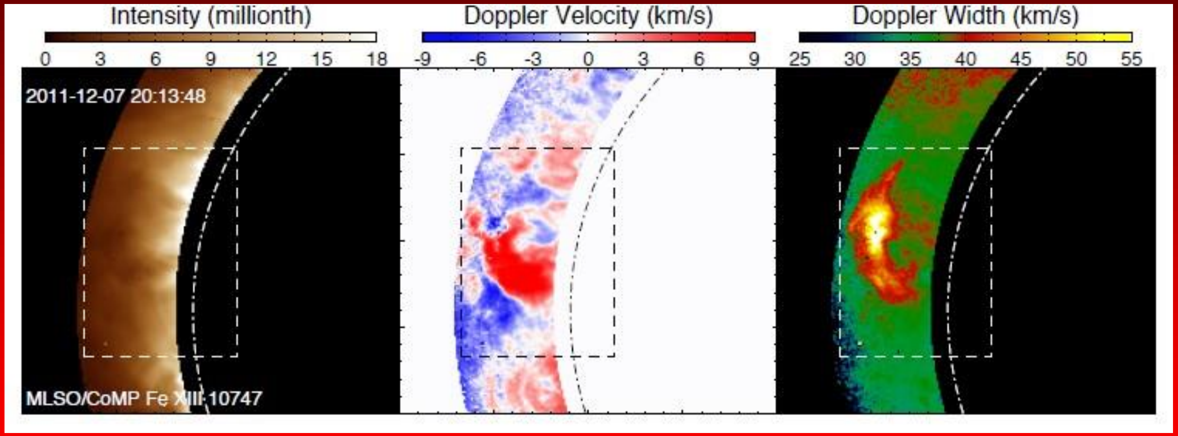

Tian et al. (2012)

SECOND PART:

determination of 3D information on CMEs from polarization-ratio technique

CME 3-D structure: multiple viewpoints

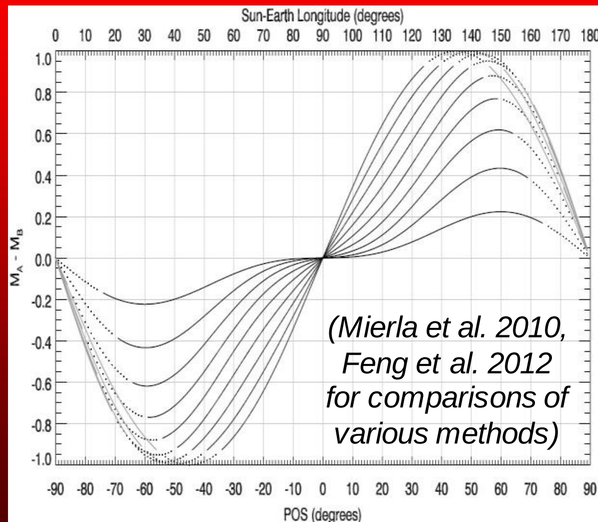

Colaninno & Vourlidas (2009)

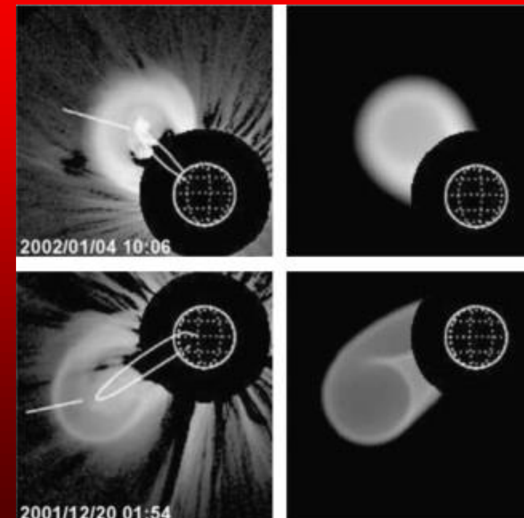

Thernisien et al. (2010)

- **tie-pointing** and **triangulation**: identification of same structures by a) visual inspection (Liewer et al. 2009; Bemporad 2009), b) local correlation tracking (Gissot et al. 2008).
- **inverse modeling:** best underlying density reproducing observations (Antunes et al. 2009)
- **constraint on the mass calculation:** (Colaninno and Vourlidas, 2009)
- **forward modeling:** empirically defined model of a flux rope (graduated cylindrical shell - GCS) → syntetic tB – pB images (Chen et al. 2000; Thernisien et al. 2006; 2009)

Results: majority of events reproduced by a "hollow croissant" model (Thernisien et al. 2009) surmounted by a hemispherical shell (Wood & Howard 2009) → CME+shock front (symmetric, radial, self-similar expansion).

CME 3-D structure: single viewpoint

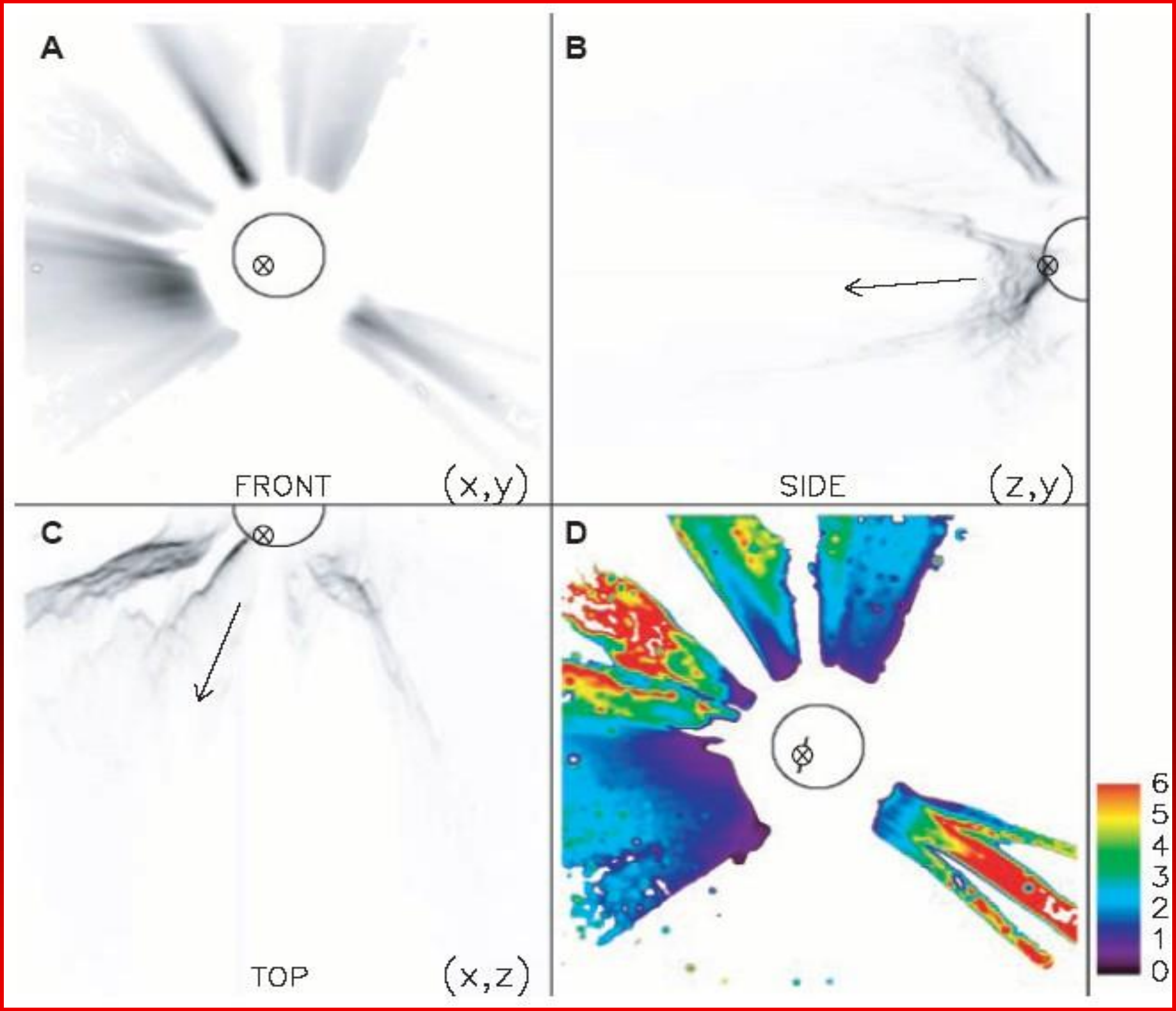

Moran & Davila (2004)

Moran & Davila (2004)

Analysis of a loop-like CME shows a complex three-dimensional structure centered at 40° from the plane of the sky, moving radially at 250 kilometers/second. Reconstruction of two halo CMEs suggests that these events are expanding loop arcades.

This is the **only existing technique** to get measurements of the **3D structure of halo CMEs from a single viewpoint**.

CME 3-D structure: single viewpoint

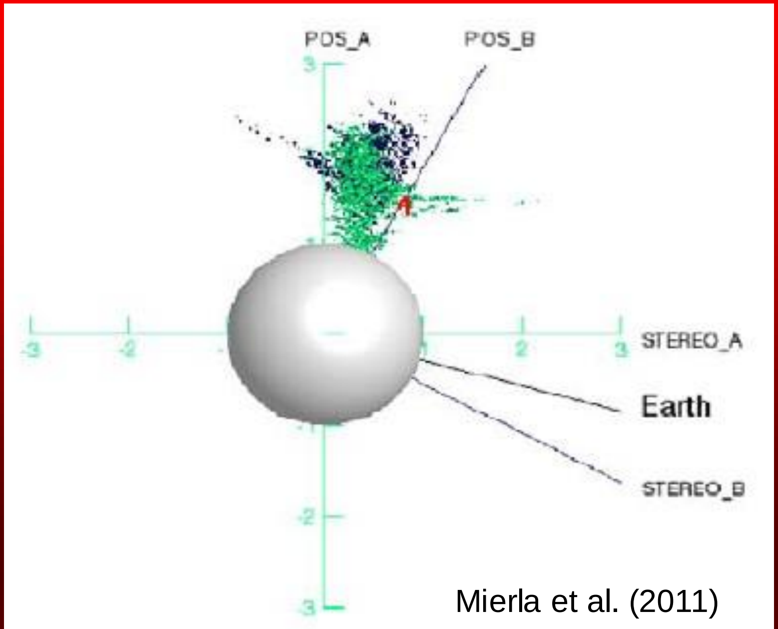

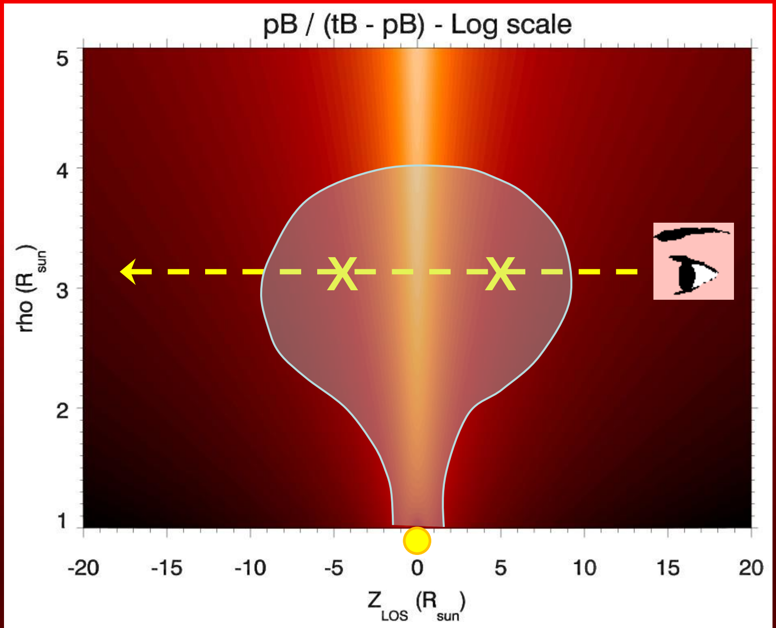

Degree of polarization of Thomson-scattering depends on scattering angle (Billings 1966) → single view-point pB-tB images contain information on CME 3-D structure → **polarization ratio technique** (Crifo et al. 1983 - validated with STEREO Moran 2010)

Results: CMEs have a **complex structure** similar to a loop arcade system (Moran & Davila 2004), filaments around a single flux rope (Dere et al. 2005) → **flux rope structure not always present**. Erupting filament not centered within overlying envelope (Moran et al. 2010).

Limits: ± z ambiguity, only LOS mass-averaged z values, for COR1 Hα 6563Å emission to be considered (Mierla et al. 2011).

Polarization ratio technique: 2D numerical test

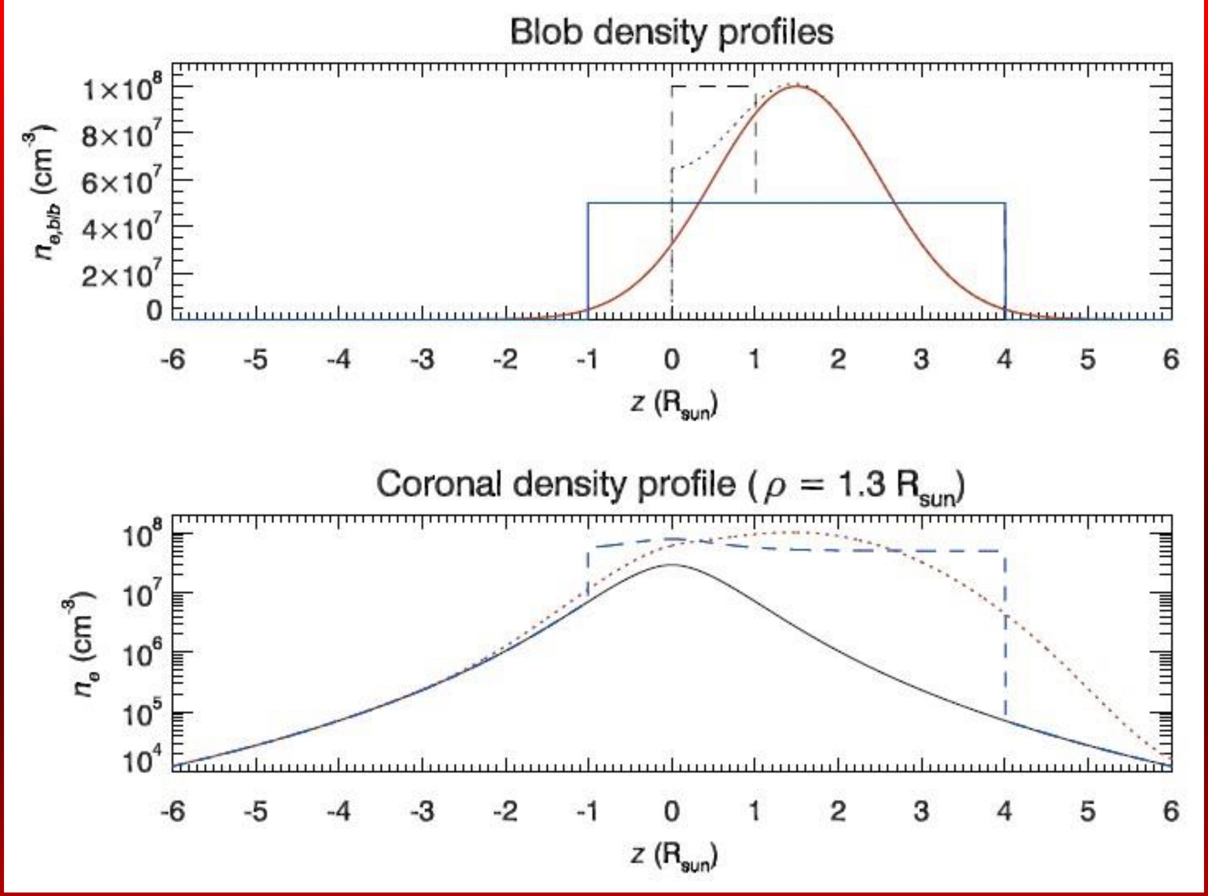

(Bemporad & Pagano 2015)

Top: blob density distribution $n_{e;blb}$ along the LOS coordinate *z* for the case (A) of constant density (solid blue line) and the case (B) of gaussian density distribution (solid red line).
Bottom: coronal density distribution $n_{e;cor}$ along the LOS (solid line) and total density distributions for the cases A (dashed blue line) and B (dotted red line).

Polarization ratio technique: 2D numerical test

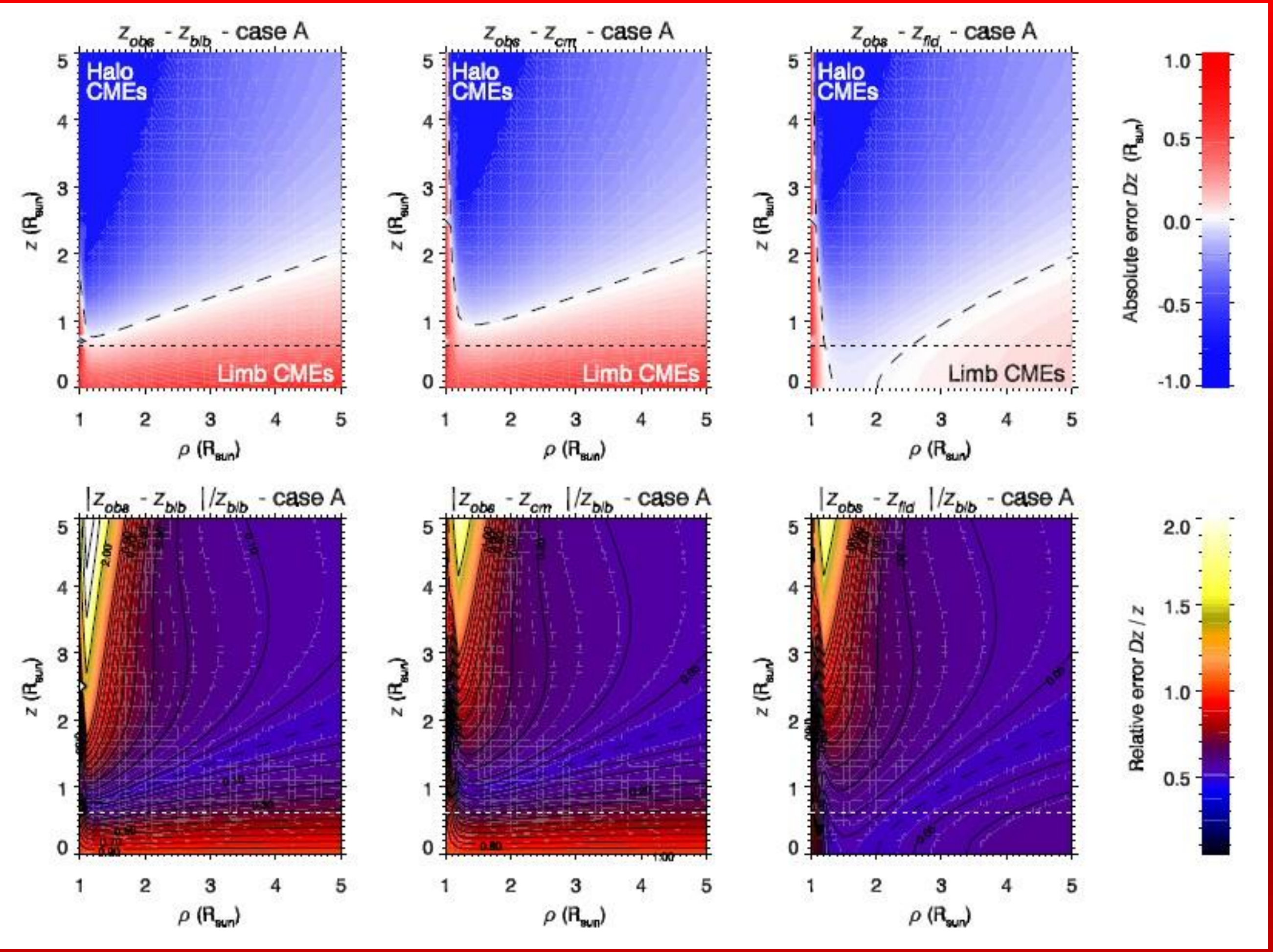

(Bemporad & Pagano 2015)

Results: the polarization ratio technique overestimates the real distance from the plane of the sky (POS) for limb CMEs. On the other hand, halo CMEs can be well characterized unless their projected altitude is too small ($< 1.5\ R_{sun}$).

Polarization ratio technique: 3D numerical test

- **3D MHD Spherical simulation** (128x128x256 pts).
- Dense and cold magnetic **flux rope formed** (by differential rotation, meridional flows and surface diffusion) **and ejected** because of initial magnetic configuration out of equilibrium.
- Coupling of Global Model (flux rope formation) + AMRVAC (CME) (Pagano et al., 2013).

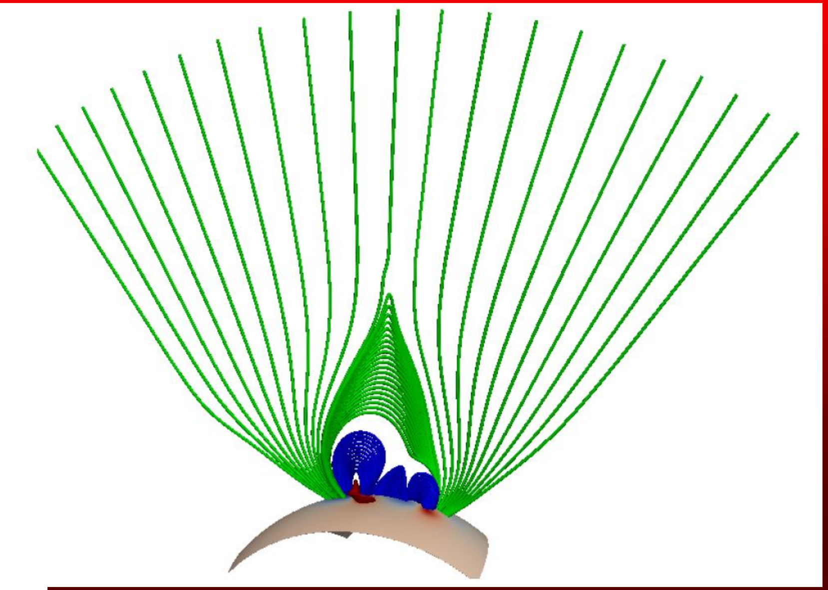

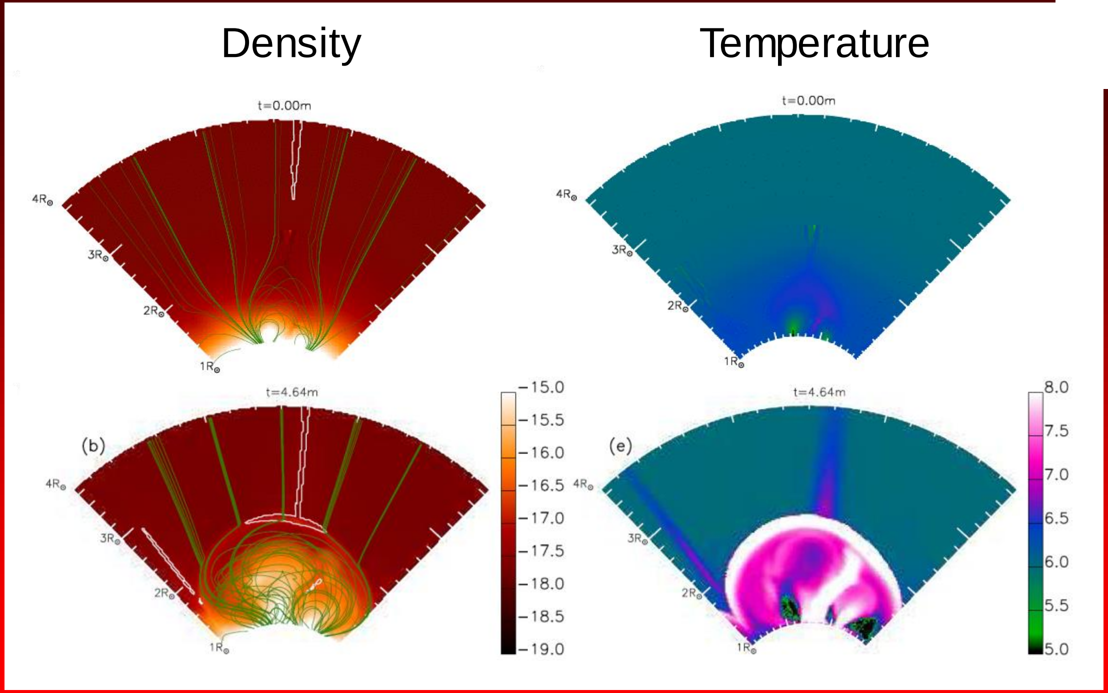

- The flux rope is ejected out of the corona, producing a **fast CME** (2000 km/s) and a propagating hot and dense front.
- The **flux rope** is initially at $10^{5.5}$ K, **is heated** (by numerical mag. diffusivity) to $10^{7.5}$ K and it finally cools down to $10^{6.2}$ K.

Reconstruction of 3D structure

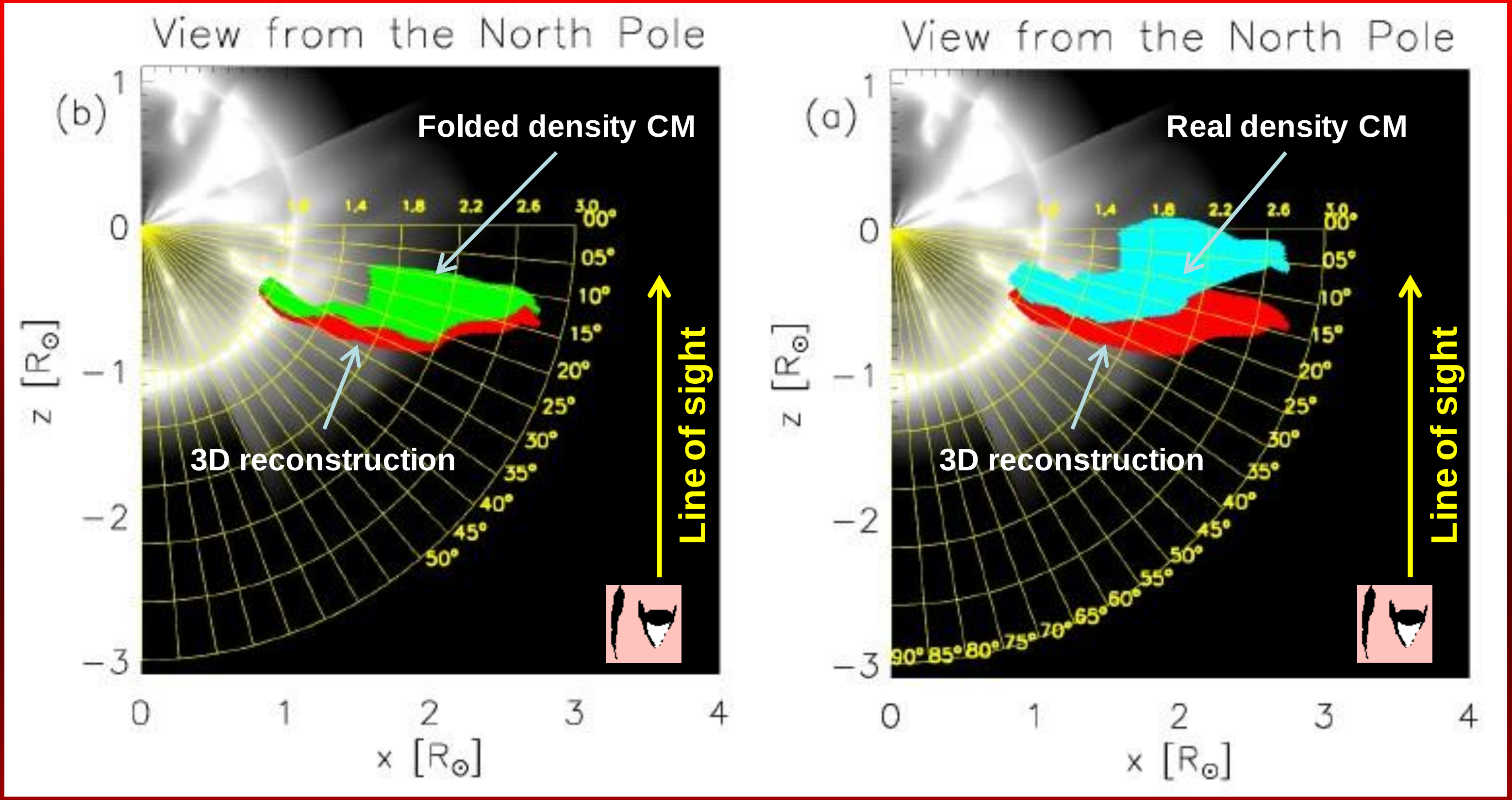

(Pagano, Bemporad & Mackay 2015)

Results: the polarization ratio technique provides a good estimate for the location along the line of sight (LOS) of what we call the folded centre of mass, namely, the centre of mass of the density distribution obtained by summing the distribution behind the plane of the sky (POS) to the one in front of it → good determination of 3D CME properties only for CMEs expanding far from the plane of the sky, like halo-CMEs.

Polarization ratio technique: 3D numerical test

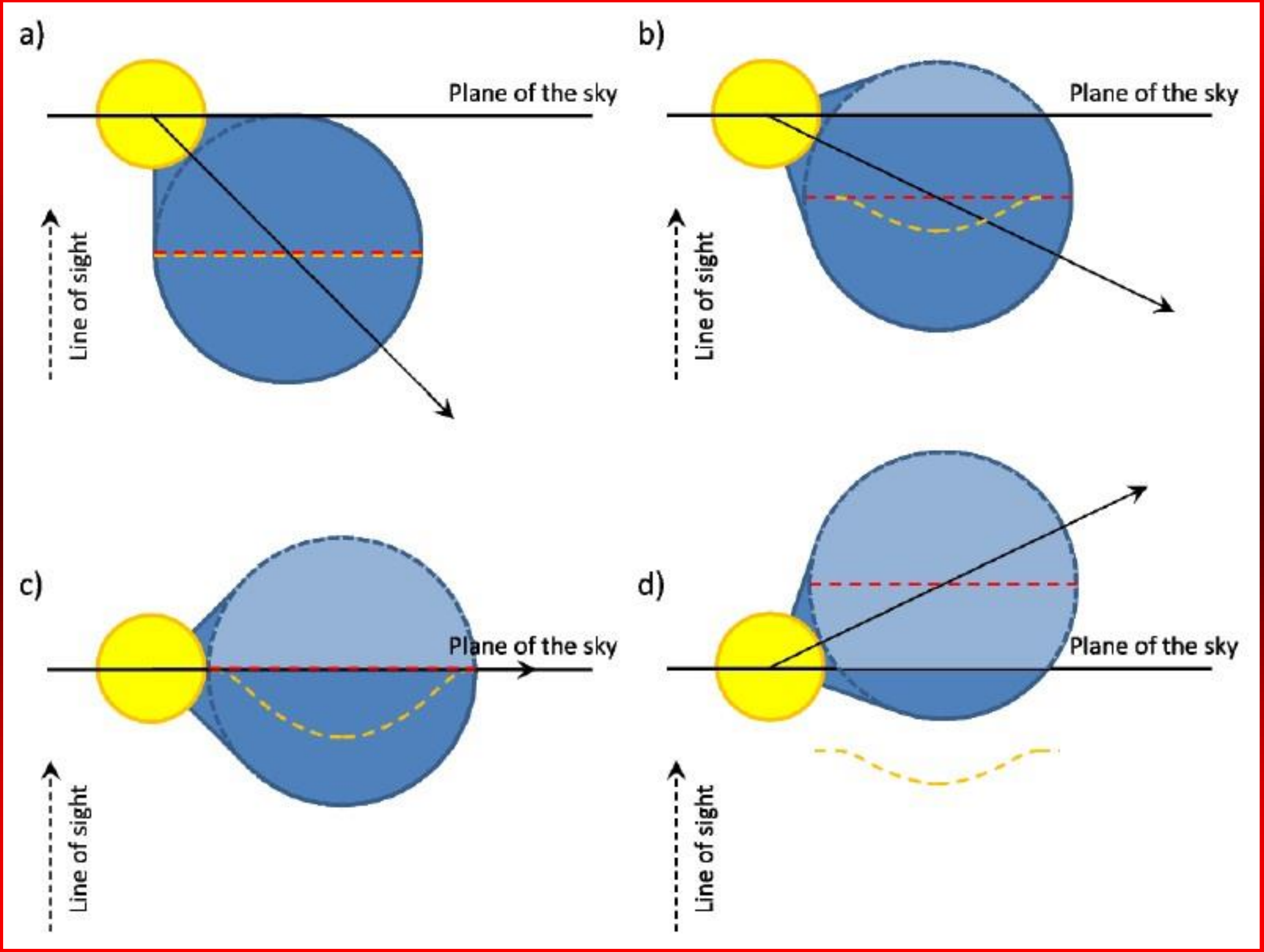

Determination of CME density/mass

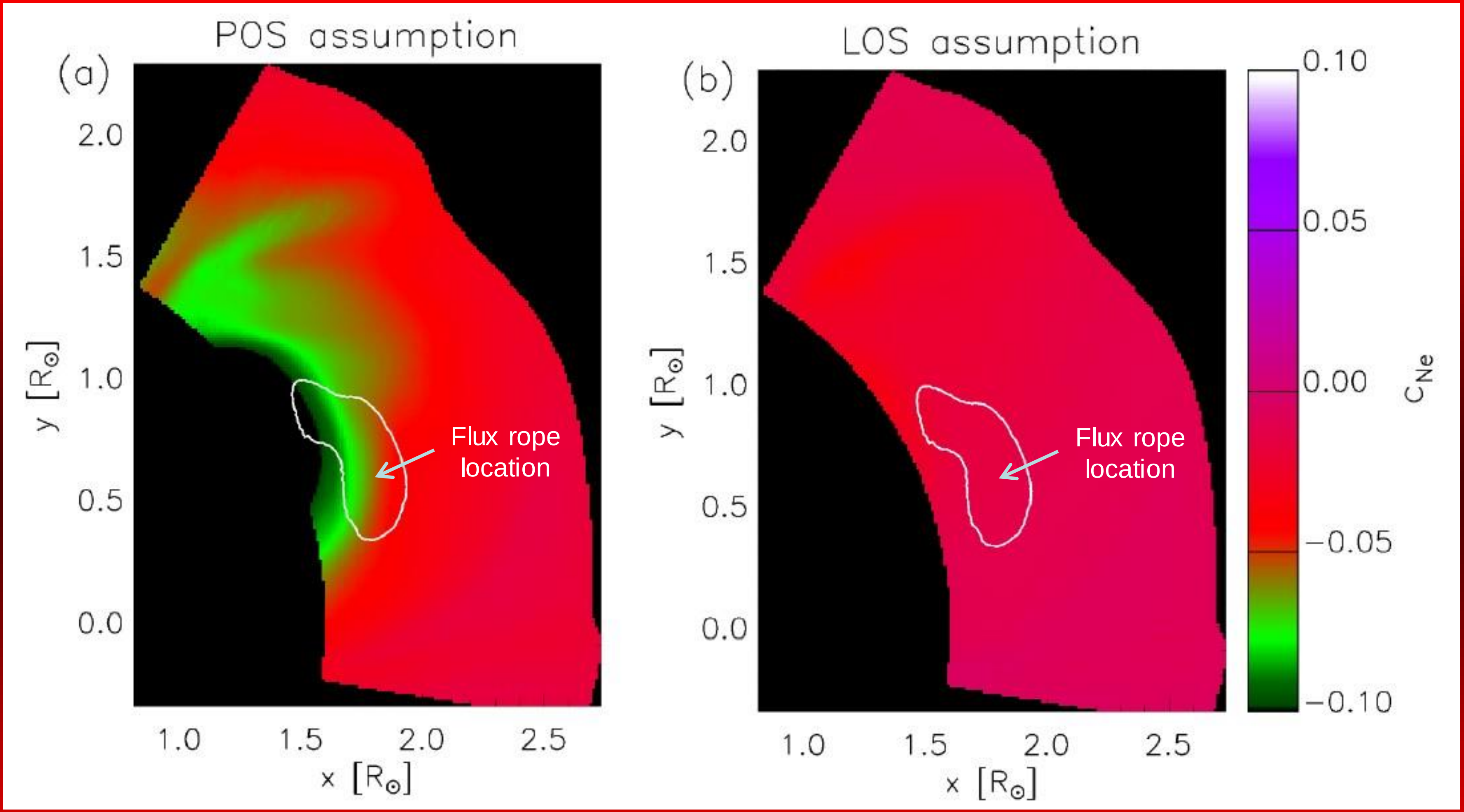

Column density measured from WL usually assumes that all electrons are on the POS → this **POS assumption** leads to an error (underestimate) of up to 10% on the column density value. In general the relative error associated with the LOS assumption is half of that associated with the POS assumption at any given location.

Reconstruction of 3D kinematic

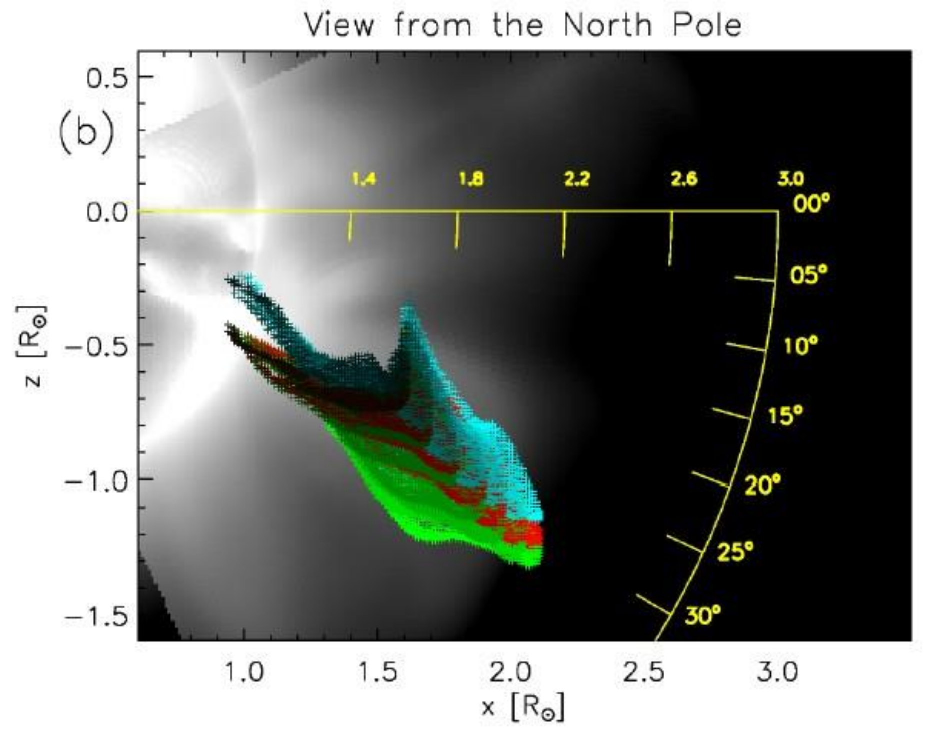

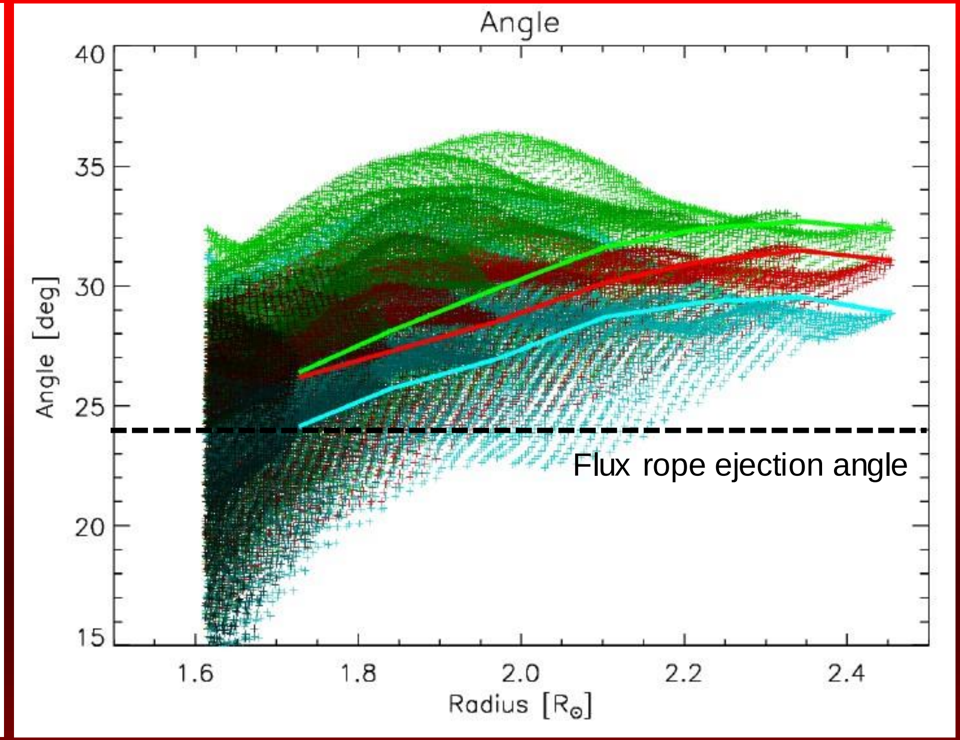

(Pagano, Bemporad & Mackay 2015)

Results: the clouds of points from the folded centre of mass (green) and from the polarization ratio technique (red) mostly coincide with a small offset that displaces the folded centre of mass slightly farther from the POS than the polarization technique.

All the clouds follow the same pattern, where the CME is deflected by ~ 5°. The trajectory of the cloud of the centre of mass (light blue) starts at ~ 24° (where the flux rope is placed) and it ends at ~ 29° → the offset between the polarization technique cloud and the centre of mass cloud leads to an **error in the CME trajectory of ~ 5°** in the longitudinal coordinate.

Future: shocks with Solar Orbiter/METIS

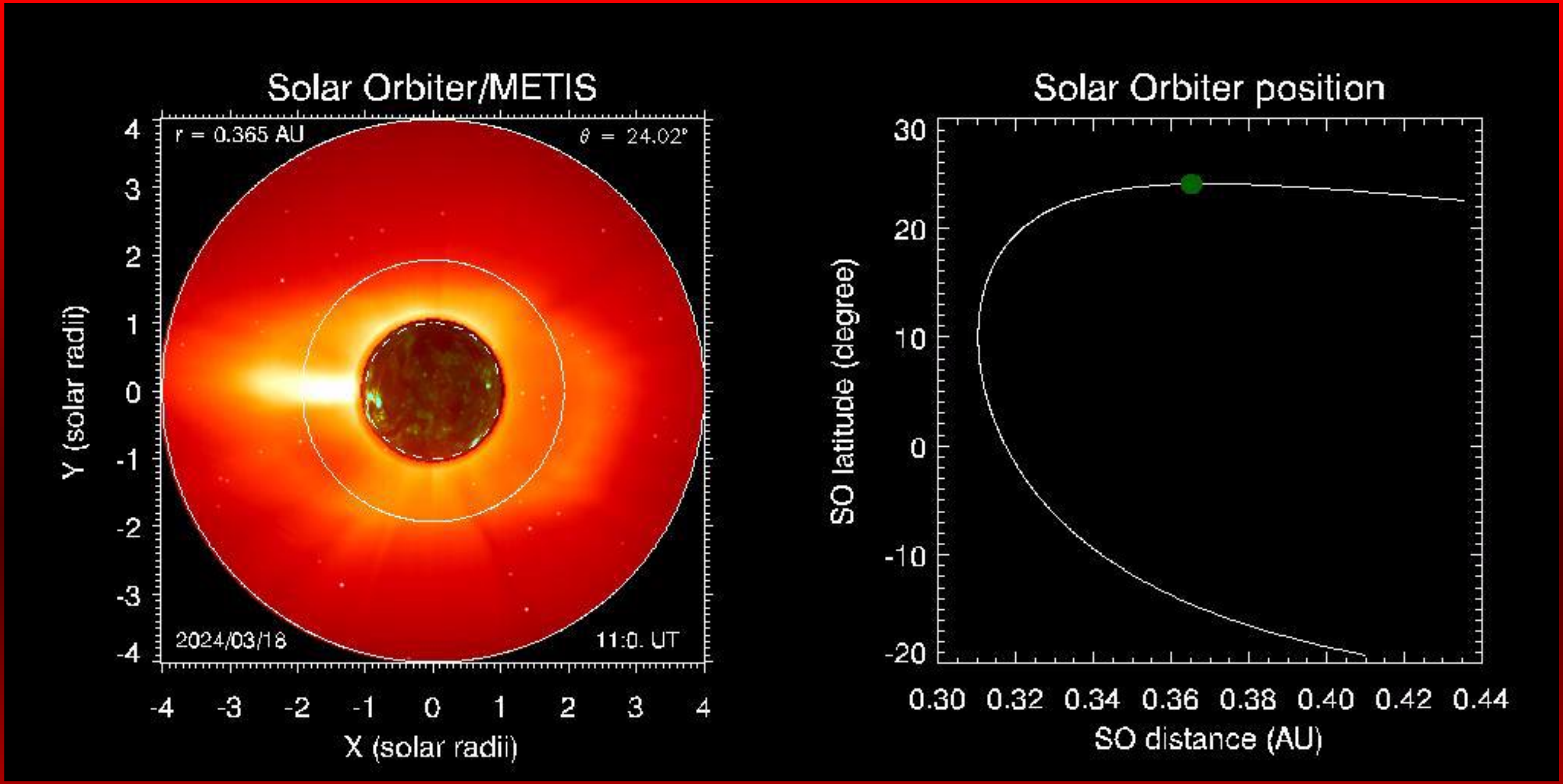

During the Solar Orbiter Mission METIS will observe coronal shocks propagating at different latitudes and over a wide range of heliocentric distances.

Shocks transit in UV → heating of protons and electrons → neutral H atoms (initially unaffected) surrounded by hotter and faster plasma → increase in collisional ionization rate by e^- and charge exchange rate with p^+ → **sudden HI Lyman-α intensity decrease** due to 1) **higher T** and 2) **higher v_{out}** (Doppler dimming) → post-shock plasma visible as **HI Ly-α dimming.**

Testing METIS CME diagnostics with simulations

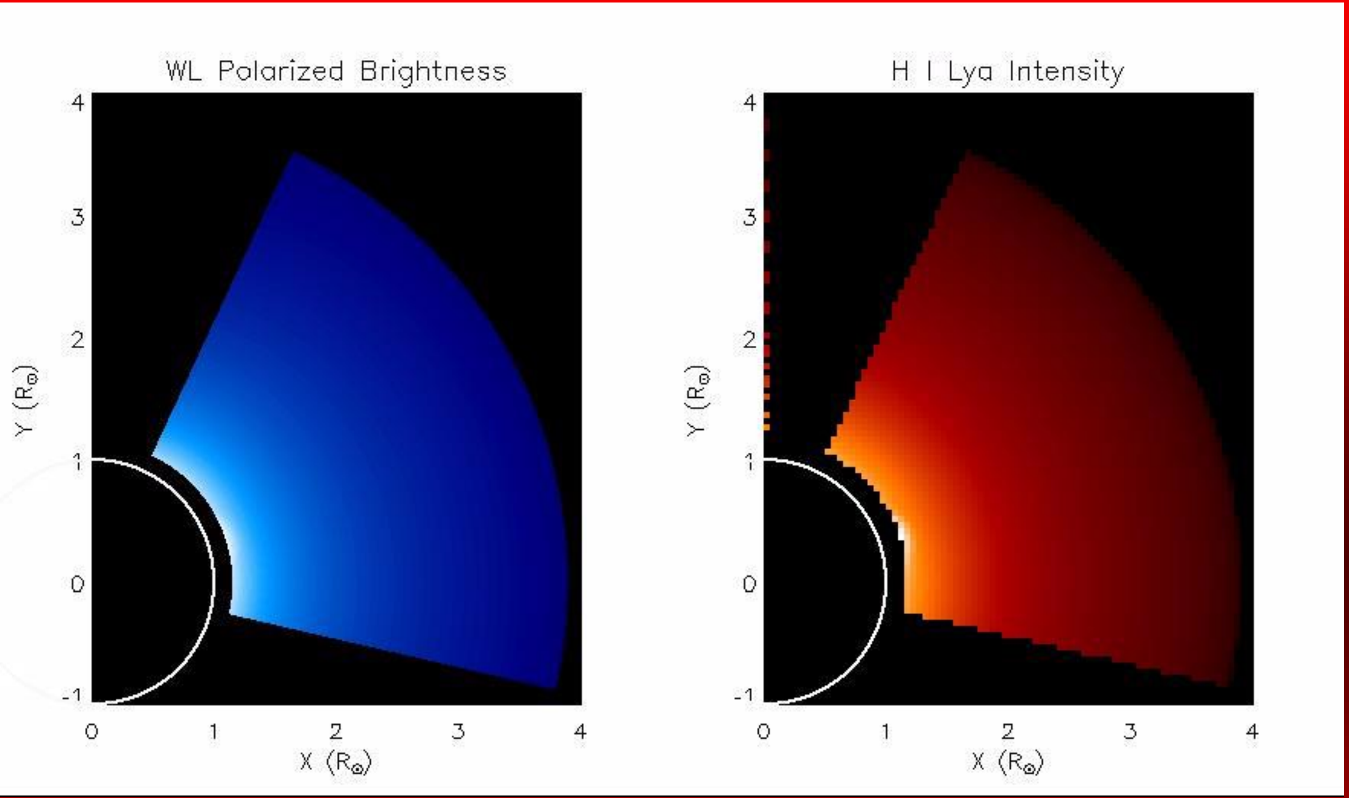

- **3D MHD simulation** performed with a flux rope expanding in a gravitationally stratified corona (**P. Pagano**)
- **Lyman-alpha emissivities** computed with density, temperature, velocity datacubes, and neglecting T anysotropies, solid angle integration, out-of-equilibrium (**S. Giordano**)

QUESTION 2: how data from next space missions will be useful to understand Space Weather?

THIRD PART:
other diagnostic capabilities
for study of solar eruptions

Prominence/CME plasma physical parameters

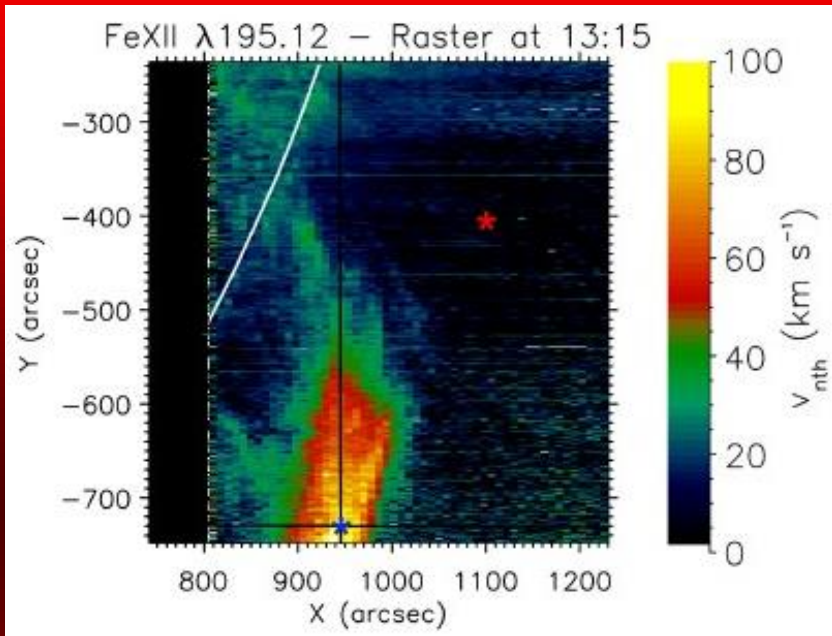

(Bemporad et al. 2009; Bemporad & Abbo 2012)

Previous experience with studies of erupting prominences and coronal holes → determination of CME plasma parameters (velocity, electron density & temperature, ion kinetic temperatures, non-thermal velocities) from EUV spectrosopic data (e.g. Hinode/EIS).

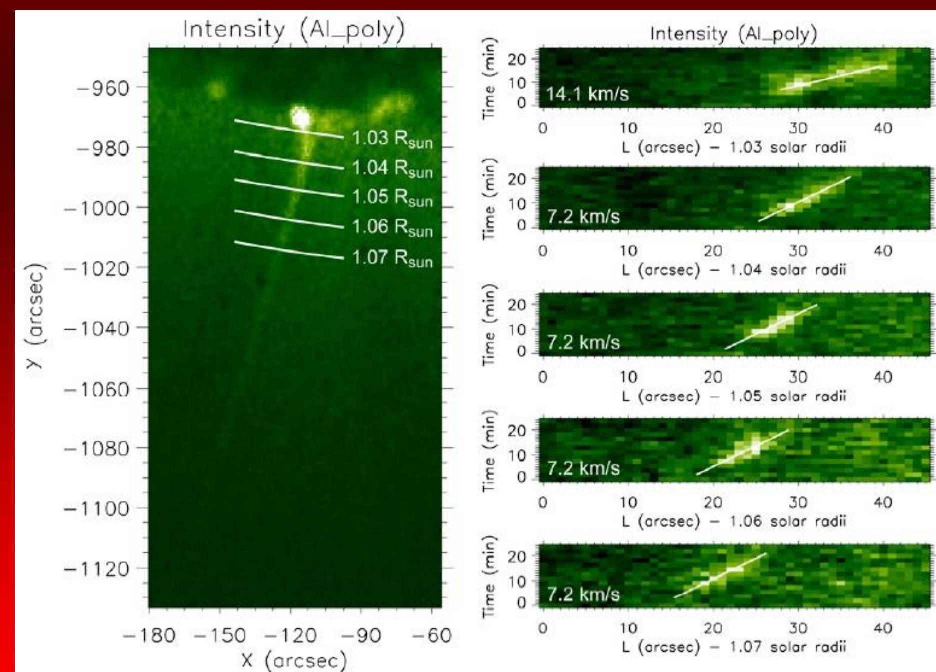

(Chandrashekhar et al. 2014; Parashiv et al. 2015)

Previous experience with studies of polar jets → determination of CME plasma parameters (velocity, electron density & temperature) from X-ray and EUV imaging data (e.g. Hinode/XRT, SDO/AIA).

Prominence/CME 3D kinematics

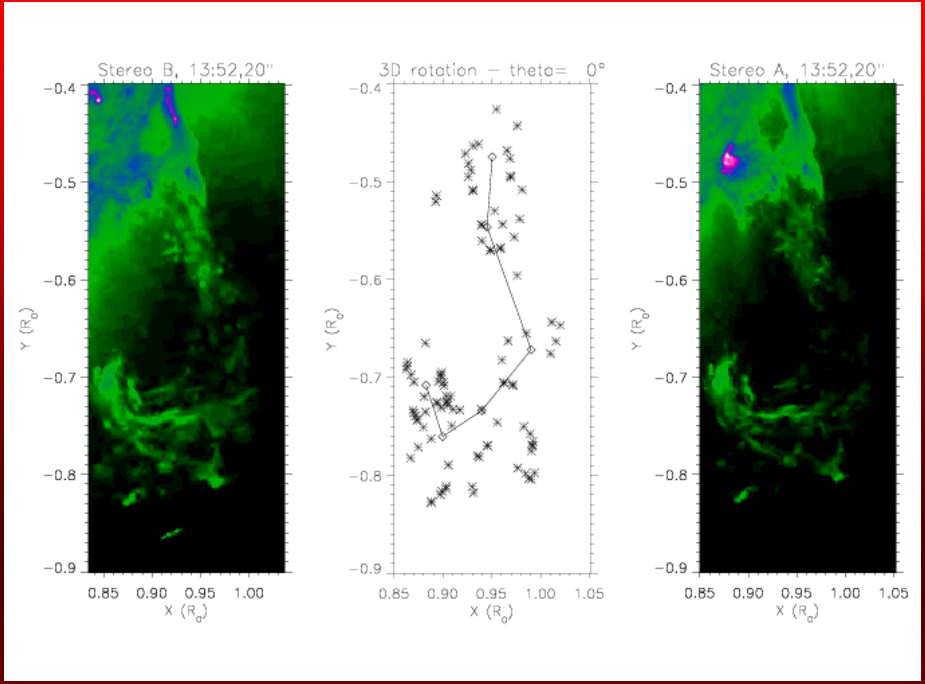

(Bemporad 2009)

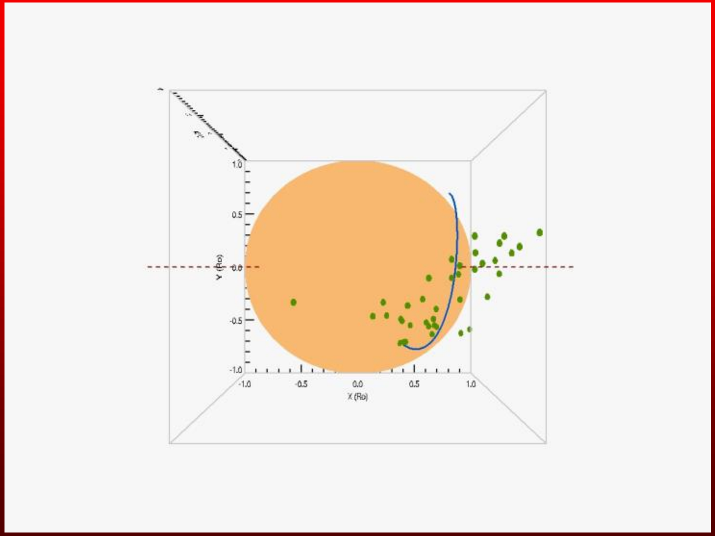

(Bemporad et al. 2012)

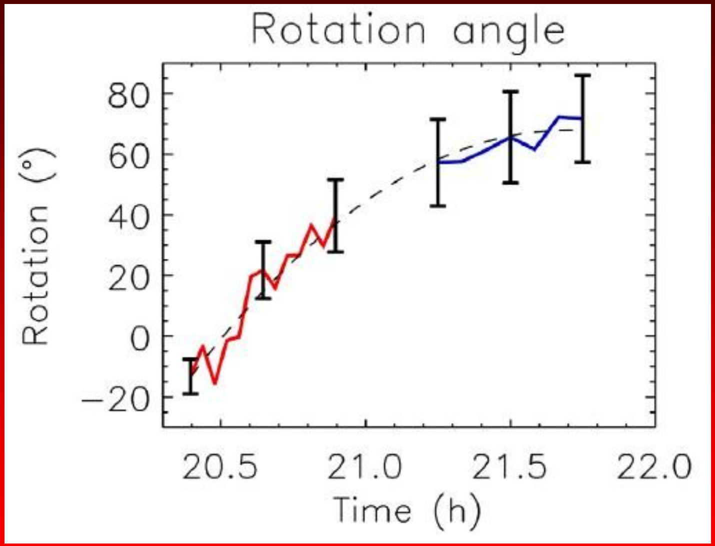

(Bemporad et al. 2011)

Previous experience 3D reconstructions with stereoscopy and polarization ratio → determination of prominence and CME plasma kinematical parameters in 3D (prominence acceleration, expansion, rotation, CME acceleration, deflection, etc…)

CME interplanetary propagation

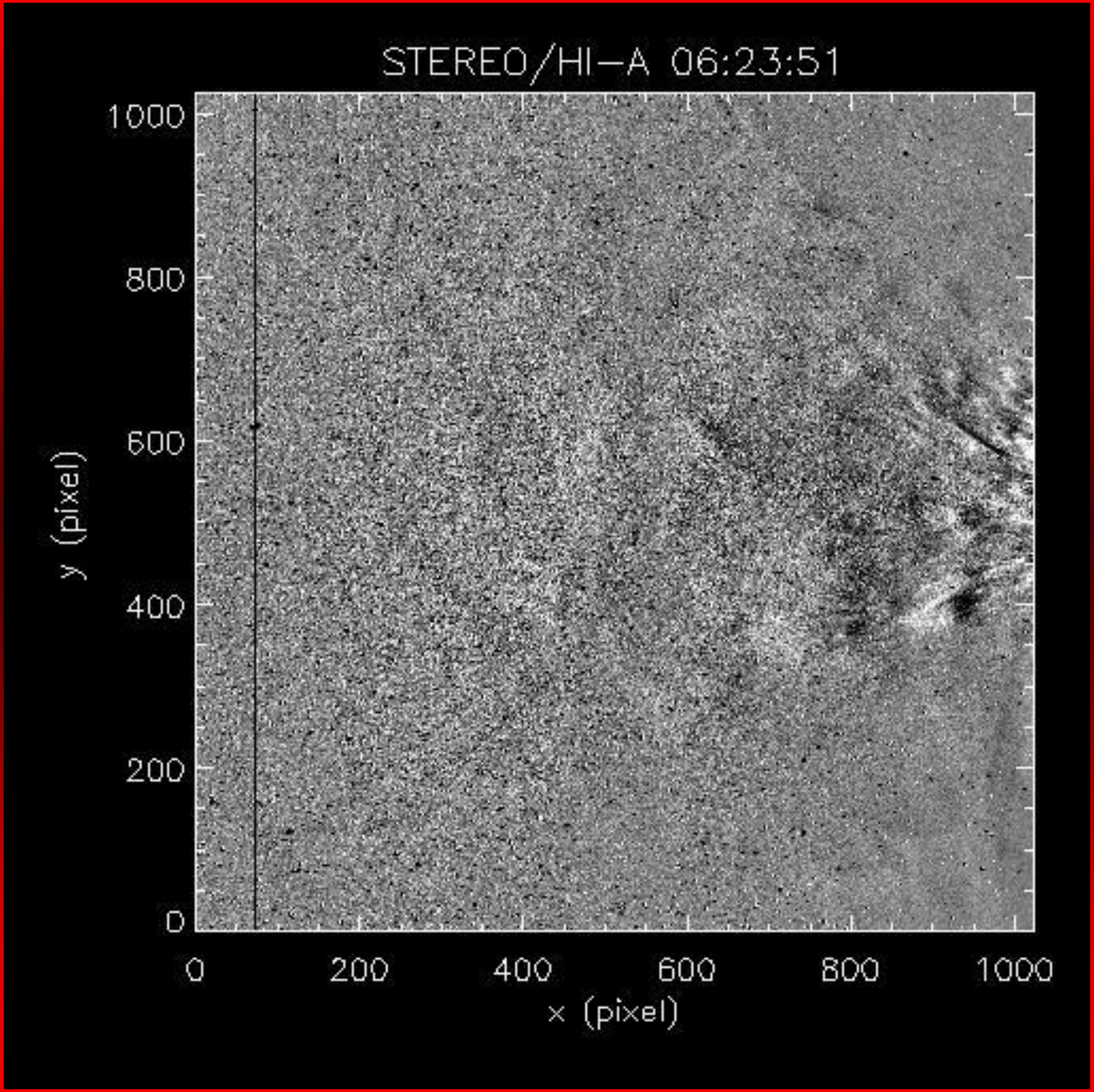

THANK YOU!